

Summer 2004

# Surface treatment of ferrous alloys with boron

Naruemon Suwattananont  
*New Jersey Institute of Technology*

Follow this and additional works at: <https://digitalcommons.njit.edu/theses>

 Part of the [Materials Science and Engineering Commons](#)

---

## Recommended Citation

Suwattananont, Naruemon, "Surface treatment of ferrous alloys with boron" (2004). *Theses*. 583.  
<https://digitalcommons.njit.edu/theses/583>

This Thesis is brought to you for free and open access by the Theses and Dissertations at Digital Commons @ NJIT. It has been accepted for inclusion in Theses by an authorized administrator of Digital Commons @ NJIT. For more information, please contact [digitalcommons@njit.edu](mailto:digitalcommons@njit.edu).

## Copyright Warning & Restrictions

The copyright law of the United States (Title 17, United States Code) governs the making of photocopies or other reproductions of copyrighted material.

Under certain conditions specified in the law, libraries and archives are authorized to furnish a photocopy or other reproduction. One of these specified conditions is that the photocopy or reproduction is not to be “used for any purpose other than private study, scholarship, or research.” If a user makes a request for, or later uses, a photocopy or reproduction for purposes in excess of “fair use” that user may be liable for copyright infringement,

This institution reserves the right to refuse to accept a copying order if, in its judgment, fulfillment of the order would involve violation of copyright law.

**Please Note: The author retains the copyright while the New Jersey Institute of Technology reserves the right to distribute this thesis or dissertation**

Printing note: If you do not wish to print this page, then select “Pages from: first page # to: last page #” on the print dialog screen



The Van Houten library has removed some of the personal information and all signatures from the approval page and biographical sketches of theses and dissertations in order to protect the identity of NJIT graduates and faculty.

## **ABSTRACT**

### **SURFACE TREATMENT OF FERROUS ALLOYS WITH BORON**

**by**

**Naruemon Suwattananont**

Boronizing is a thermo-chemical surface hardening treatment in which boron atoms diffused into the metal substrate form the metallic boride layer, providing high hardness, corrosion resistance, and 3-10 times increasing service life. This type of surface treatment is widely used in many applications.

The purpose of this work was to investigate the structures and properties of boronized ferrous alloys. Three types of steels, AISI 1018 (plain low carbon steel), AISI 4340 (high strength alloy steel), and AISI 304 (austenitic stainless steel), were used for this study. The boronized AISI 1018 and AISI 4340 demonstrated the saw-tooth structure with average 75-76  $\mu\text{m}$  and 57-58  $\mu\text{m}$  in depth, respectively. On the other hand, the narrow and flatten boride layer with average 10-11  $\mu\text{m}$  was observed in the boronized AISI 304. The microhardness of boride layer in AISI 1018 and AISI 4340 was detected in the range of 1400-2200 HV and 1800-2200 HV, respectively, while that in AISI 304 was about 400-700 HV. Moreover, boronized steels showed the improved corrosion resistance in acid and oxidation resistance at high temperature rather than unboronized steels.

# **SURFACE TREATMENT OF FERROUS ALLOYS WITH BORON**

**by**  
**Naruemon Suwattananont**

**A Thesis**  
**Submitted to the Faculty of**  
**New Jersey Institute of Technology**  
**in Partial Fulfillment of the Requirements for the Degree of**  
**Master of Science in Materials Science and Engineering**

**Interdisciplinary Program in Materials Science and Engineering**

**August 2004**



**APPROVAL PAGE**

**SURFACE TREATMENT OF FERROUS ALLOYS WITH BORON**

**Naruemon Suwattananont**

Dr. Roumiana S. Petrova, Dissertation Advisor  
Special Lecturer of Physics, NJIT

Date

Dr. Roland A. Levy, Committee Member  
Distinguished Professor of Physics, ~~NJIT~~

Date

~~Dr. John Federici, Committee Member  
Professor of Physics, NJIT~~

Date

## BIOGRAPHICAL SKETCH

**Author:** Naruemon Suwattananont

**Degree:** Master of Science

**Date:** August 2004

### **Undergraduate and Graduate Education:**

- Master of Science in Materials Science and Engineering,  
New Jersey Institute of Technology, Newark, NJ, 2004
- Master of Science in Materials Science (Ceramic Technology),  
Chulalongkorn University, Bangkok, Thailand, 1996
- Bachelor of Science in Chemistry,  
Chiang Mai University, Chiang Mai, Thailand, 1993

**Major:** Materials Science and Engineering



**To my beloved family for their love, encouragement and support  
especially, for their understanding in the way I am.**

## **ACKNOWLEDGMENT**

I would like to express my deepest appreciation to my advisor, Dr. Roumiana S. Petrova, who gave me the opportunity to do this thesis and spent her time and offered for many suggestions during the entire study. Special thanks are given to Dr. Roland A. Levy and Dr. John Federici for actively participating in my committee.

Appreciation is also extended to all professors, graduate students and staff of Physics Department, New Jersey Institute of Technology.

I would like to express my gratitude to my family and boyfriend for their love, patience and encouragement and also my appreciation for the research financial support from U.S. Army ARDEC, Picatinny Arsenal, New Jersey.

## TABLE OF CONTENTS

<b>Chapter</b>	<b>Page</b>
1 INTRODUCTION.....	1
1.1 Objective.....	1
1.2 Background Information.....	1
1.3 The Trend of Surface Treatment with Boron.....	2
2 BORONIZING.....	6
2.1 Boronizing (Boriding).....	6
2.2 Boronizing of Ferrous Materials.....	7
2.3 Boronizing of Nonferrous Materials.....	9
2.4 The Mechanism of Boronizing Process.....	10
2.5 Effects of Alloying Elements.....	11
2.6 Advantages and Disadvantages of Boronizing.....	13
2.7 Application of Boronized Products.....	16
3 BORONIZING PROCEDURE.....	17
3.1 Pack Boronizing.....	17
3.2 Paste Boronizing.....	18
3.3 Liquid Boronizing.....	18
3.4 Gas Boronizing.....	19
3.5 Plasma Boronizing.....	20
3.6 Fluidized Bed Boronizing.....	20
3.7 Multi-component Boronizing.....	21

**TABLE OF CONTENTS**  
**(Continued)**

<b>Chapter</b>	<b>Page</b>
4 PROPERTIES OF BORONIZED STEELS.....	23
4.1 Toughness.....	23
4.2 Adhesion Resistance.....	23
4.3 Adhesive Wear Resistance.....	23
4.4 Corrosion Resistance in Acids.....	25
5 EXPERIMENTAL PARTS.....	26
5.1 Description of Experiments.....	26
5.2 Experimental Procedures.....	27
5.2.1 Sample Preparation.....	27
5.2.2 The Procedure of Boronizing Heat Treatment.....	27
5.2.3 Characterization of Boride Layers.....	29
5.2.4 Corrosion Testing.....	31
5.2.5 Oxidation Resistance Testing.....	32
6 RESULTS AND DISCUSSION.....	33
6.1 Characteristics of Boride Layer.....	33
6.1.1 Boride Layer.....	33
6.1.2 Phases Present in the Boride Layer.....	34
6.1.3 The Morphology and Thickness of Boride Layer.....	37
6.1.4 Microhardness.....	39
6.2 Corrosion Testing.....	40

**TABLE OF CONTENTS**  
**(Continued)**

<b>Chapter</b>	<b>Page</b>
6.3 Oxidation Resistance Testing.....	42
7 CONCLUSION.....	44
8 FUTURE WORK.....	45
APPENDIX A Fe-B PHASE DIAGRAM.....	46
APPENDIX B Fe <sub>2</sub> B XRD DATA.....	47
APPENDIX C FeB XRD DATA.....	49
REFERENCES.....	51

## LIST OF TABLES

<b>Table</b>		<b>Page</b>
2.1	The Microhardness and Constitution of Boride Layers on Various Substrates Formed after Boronizing.....	7
2.2	The Surface Hardness of Boronized Steels Compares to Other Treatments and Hard Materials.....	15
2.3	The Application of Boronized Ferrous Materials.....	16
3.1	The Multi-Component Boronizing.....	21
5.1	The Chemical Composition of Steel Samples.....	27
5.2	The Grinding and Polishing Procedure for the Steel Substrates.....	30
6.1	The Boride Phase on the Specimen Surface.....	35
6.2	The Boride-layer Thickness on Steel Substrate.....	37

## LIST OF FIGURES

Figure		Page
2.1	The saw-tooth structure of boride layers with exterior layer FeB and interior layer Fe <sub>2</sub> B of AISI 1018.....	8
2.2	The effect of steel composition on the morphology and thickness of the boride layer.....	11
2.3	The effect of percent alloying elements on the boride layer thickness.....	12
2.4	The hardness value for various materials and surface treatments.....	15
4.1	The effect of steel composition (nominal values in wt %) on wear resistance under abrasive wear ( $d_v$ = thickness of the boride layer).....	24
4.2	The comparison of wear resistance between boronized steels and non-boronized steel.....	24
4.3	The comparison of corrosion resistance between boronized steels and non-boronized steels.....	25
5.1	The experimental description flow chart.....	26
5.2	The equipment setting for corrosion testing (continuous weighting method).....	32
6.1	The image of AISI 1018 specimen surface before and after boronizing.....	33
6.2	The image of AISI 4340 specimen surface before and after boronizing.....	34
6.3	The image of AISI 304 specimen surface before and after boronizing.....	34
6.4	The XRD pattern of AISI 1018 before and after boronizing (P-unboronized Specimen, B-boronized specimen).....	35
6.5	The XRD pattern of AISI 4340 before and after boronizing (P-unboronized specimen, B-boronized specimen).....	36
6.6	The XRD pattern of AISI 304 before and after boronizing (P-unboronized specimen, B-boronized specimen).....	36

**LIST OF FIGURES**  
**(Continued)**

<b>Figure</b>	<b>Page</b>
6.7 The saw-tooth morphology and the distribution of the boride-layer thickness on AISI 1018.....	37
6.8 The saw-tooth morphology and the distribution of the boride-layer thickness on AISI 4340.....	38
6.9 The saw-tooth morphology and the distribution of the boride-layer thickness on AISI 304.....	38
6.10 The plot between the microhardness and the depth of boride layer in AISI 1018.....	39
6.11 The plot between the microhardness and the depth of boride layer in AISI 4340.....	39
6.12 The plot between the microhardness and the depth of boride layer in AISI 304.....	40
6.13 The corrosion tests of unboronized and boronized specimen (AISI 1018) in HCl solution (B- boronized specimen, P-unboronized specimen).....	41
6.14 The corrosion tests of unboronized and boronized specimen (AISI 4340) in HCl solution (B- boronized specimen, P-unboronized specimen).....	41
6.15 The corrosion tests of unboronized and boronized specimen (AISI 304) in HCl solution (B- boronized specimen, P-unboronized specimen).....	41
6.16 The oxidation test of boronized and unboronized specimen (AISI 1018) at 600 °C for 12 hours (B- boronized specimen, P-unboronized specimen).....	42
6.17 The oxidation test of boronized and unboronized specimen (AISI 4340) at 600 °C for 12 hours (B- boronized specimen, P-unboronized specimen).....	43
6.18 The oxidation test of boronized and unboronized specimen (AISI 304) at 600 °C for 12 hours (B- boronized specimen, P-unboronized specimen).....	43
A.1 B-Fe (Boron-Iron) phase diagram.....	46



# CHAPTER 1

## INTRODUCTION

### 1.1 Objective

The purpose of this work is to study the processing and characteristics of boronized steels. Three types of steel, AISI 1018, AISI 4340, and AISI 304, are investigated. AISI 1018, plain low carbon steel, is widely utilized in many applications due to the low cost; therefore, after boronizing the steel properties are improved beneficial to the industry. Like AISI 1018, AISI 4340, high strength alloy steel, is chosen to study due to the need of better properties in aerospace industries. Finally, AISI 304, austenitic stainless steel (18Cr8Ni), is used to compare the results of boronized AISI 1018 and boronized AISI 4340, according to general uses in the industries and good properties in corrosion and oxidation at high temperature.

### 1.2 Background Information

Boronizing is a well-known thermo-chemical surface hardening treatment today. The boron atoms diffused into the metal substrate can form the metallic boride layer on the metal surface, providing high hardness, corrosion resistance, and 3-10 times increasing service life <sup>[1]</sup>. Boronizing can complement the technology gap between conventional heat treatment and chemical/physical vapor deposition; therefore, it is used to replace many applications in carburizing, nitriding, and carbonitriding <sup>[2]</sup>. However, only the pack and paste boronizing techniques are able to process in many applications while

other techniques, such as the liquid and gas boronizing techniques, are incapable of the application because of toxicity problems.

Furthermore, the process can be applied to the irregular surfaces or the specific areas of a surface. The high-volume production applications are also available to process as first demonstrated in the European automotive industry <sup>[3]</sup>. As mentioned earlier, boronizing fills out the gap between low and high technology; hence the process provides low procedure cost but high quality products, which is beneficial for the commercial section. In addition, boronizing can combine with other heat treatments to produce the multi-component boride layers that have the better properties. The combination of excellent wear resistance, corrosion resistance in acid, and oxidation resistance at high temperature is one of the attractive features for the industrial application.

### **1.3 The Trend of Surface Treatment with Boron**

The trend of surface treatment with boron can be classified into three categories:

#### **1. The advanced boronizing techniques**

In the last ten years, the novel techniques were used to produce an efficient boride layer on the substrate surface as discussed below:

The laser surface modification <sup>[4]</sup> was used to form the boride layer on 41Cr4 medium carbon steel. Although this method reduced the hardness of the boride layer, it reduced the hardness gradient between the boride layer and substrate. As a result, it caused the increasing wear resistance in comparison with that of the conventional method.

The fluidized bed reactor was used to form the boride coating 0.5%wt. C steel <sup>[5]</sup>, nickel alloy <sup>[6]</sup>, and nonferrous materials <sup>[7]</sup>. For this method, the process could get the adequate thickness and improved wear and oxidation resistances.

Plasma Transferred Arc process (PTA) technique, with using boron and chromium diboride powders, was used to form iron-boron <sup>[8]</sup> and iron-chromium-boron <sup>[9]</sup> coatings. Both coatings presented high hardness and excellent wear resistance.

Spark Plasma Sintering (SPS) technique <sup>[10]</sup> was able to avoid the drawbacks of pack boronizing that took several hours during the boronizing and of plasma-assisted boronizing that provided a high degree of porosity on the boride layer.

The plasma-assisted boronizing of ferrous materials was formed under  $\text{BCl}_3\text{-H}_2\text{-Ar}$  atmosphere <sup>[11]</sup>. The treatment parameters and discharge conditions helped eliminating the porosity of the boride layer. The plasma activation of  $\text{Ar-H}_2\text{-BF}_3$  atmosphere was also used to avoid the processing corrosion <sup>[12]</sup>.

The D.C.-plasma boronizing technique combined with PVCVD process achieved the deposition of boride layer at low temperature (873 K) <sup>[13]</sup>.

The plasma paste boronizing <sup>[14]</sup> technique was processed on AISI 304. The boronizing paste had consisted of amorphous boron and borax under gas mixture of  $\text{Ar:H}_2$  (2 : 1).

The ion implantation technique was processed on iron and AISI M2 steel along with using a high current density, low-energy, and broad-beam ion source <sup>[15]</sup>. The process provided thick boride layer while the boronizing temperature was at 600 °C for iron and at 700 °C for steel.

## 2. The conventional boronizing technique

In spite new boronized techniques have been studied, many conventional techniques, such as pack boronizing and salt bath, are still widely used to study on many steels and their properties: in ductile iron <sup>[16]</sup>, AISI W1 steel <sup>[17]</sup>, AISI 316L stainless steel <sup>[18]</sup>, AISI W4 steel <sup>[19]</sup>, WC-Co steel <sup>[20]</sup>, 99.5% purity nickel <sup>[21]</sup>, chromium-based low alloy steels <sup>[22]</sup>, and etc.

## 3. Multi-component surface treatment

The multi-component of boronizing has widely been studied to improve the mechanical properties, corrosion, and oxidation resistances:

Chromizing and boronizing treatment was combined to increase the high oxidation resistance <sup>[23]</sup>.

Boro-nitriding of steel US 37-1 <sup>[24]</sup> was studied by combining two processes of pack boronizing and gas nitriding to produce the boride, nitride and boro-nitride layer with pore-free and excellent adherence.

Vanadium boride coatings on steel <sup>[25]</sup> consisted of the thermo-diffusion of vanadium and followed by boron. The microhardness of  $VB_2$  was at 23600 MPa.

B-C-nitriding in a two-temperature-stage process was achieved to improve the boronizing embrittlement <sup>[26]</sup>. The complex (B- C- N) diffusion layers (borocarbonitrided layer) <sup>[27]</sup> were formed on chromium and nickel-based low-carbon steel. Despite the Borocarbonitriding reduced the depth of iron boride zone, it decreased microhardness gradient across the layer so that it resulted in the low brittleness of the boride layer.

The two-step treatment carburizing followed by boronizing on medium-carbon steel was found to increase wear resistance and to decrease microhardness gradient <sup>[28]</sup>.

The simultaneous boronizing and aluminizing produced under the gas phase reaction of paste mixtures <sup>[29]</sup> was studied. The boroaluminized layers of C3, C5XHM, X12, and X18H9T steels <sup>[30]</sup> were investigated. The resulting complex diffusion layers could be separated into three groups: the needle-shaped layer with aluminium dissolved into iron boride, the layer showing conglomerates of boride and aluminium phases, and the layer with rich aluminium phases on the external surface.

The one-step boroaluminizing heat treatment was studied on 2.25Cr–Mo steel <sup>[31]</sup> by means of pack cementation technique using a B/Al boronizing powder. Three distinct regions were found in the coatings: first, an outer Al-rich layer region, second, a transition region containing Al and Fe, and third, an inner layer region containing mostly B and Fe. The boroaluminizing improved the oxidation and hot corrosion resistance.

The multi-component of  $\text{Ni}_4\text{B}_3$ ,  $(\text{Fe,Ni})\text{B}$ , and  $(\text{Fe,Ni})_2\text{B}$  borides <sup>[32]</sup> was produced by combining the electrochemical nickel deposition and plasma boronizing to increase the wear and corrosion resistance of surface.

## **CHAPTER 2**

### **BORONIZING**

#### **2.1 Boronizing (Boriding)**

Boronizing is a thermo-chemical surface hardening process that boron atoms diffuse into a base metal (steel) and form the hard metallic boride layer on the surface. The process can be applied to both ferrous and nonferrous materials by heating well-cleaned materials in the temperature range of 700 - 1000°C (1300 - 1830°F) for several hours. The process provides the metallic boride layer about 20-300  $\mu\text{m}$  thick. The resulting metallic boride layer yields the outstanding properties of high hardness, good wear and corrosion resistance, and moderate oxidation resistance at high temperature. Although many metals and alloys can be boronized, aluminium and magnesium alloys cannot be boronized due to their low melting points. In addition, copper alloy is unable to form the stable boride phase <sup>[33]</sup>.

During boronizing, boron atoms diffuse and subsequently absorb into the metallic lattice of the component surface. As a result, an interstitial boron compound is formed with either a single-phase boride or a poly-phase boride layer. Several characteristics of the boride layer, including the morphology, the growth, and the phase composition, depend on the elements in the substrate materials (Table 2.1).

**Table 2.1** The Microhardness and Constitution of Boride Layers on Various Substrates Formed after Boronizing<sup>[33]</sup>

Substrate	Constituent phases in the boride layer	Microhardness of layer, HV or kg/mm <sup>2</sup>
Fe	FeB	1900-2100
	Fe <sub>2</sub> B	1800-2000
Co	CoB	1850
	Co <sub>2</sub> B	1500-1600
Co-27.5 Cr	CoB	2200 (100 g)
	Co <sub>2</sub> B	~1550 (100 g)
Ni	Ni <sub>4</sub> B <sub>3</sub>	1600
	Ni <sub>2</sub> B	1500
	Ni <sub>3</sub> B	900
Inco 100	...	1700 (200 g)
Mo	Mo <sub>2</sub> B	1660
	Mo <sub>2</sub> B <sub>5</sub>	2400-2700
W	W <sub>2</sub> B	~2700 (overall hardness)
	WB	
	W <sub>2</sub> B <sub>5</sub>	
Ti	TiB	2500
	TiB <sub>2</sub>	3370
Ti-6Al-4V	TiB	3000 (100 g) (overall hardness)
	TiB <sub>2</sub>	
Nb	Nb <sub>2</sub> B <sub>2</sub>	2600-3000 (overall hardness)
	NbB <sub>4</sub>	
Ta	Ta <sub>2</sub> B	3200-3500
	TaB <sub>2</sub>	2500
Zr	ZrB <sub>2</sub>	2300-2600 (overall hardness)
	Zr <sub>2</sub> B	
Re	ReB	2700-2900

## 2.2 Boronizing of Ferrous Materials

The boride layer formed on iron and steel can be of either a single phase or double-phase, corresponding to a definite composition from Fe-B phase diagram (Appendix A). Fe<sub>2</sub>B is obtained for the single-phase layer, while the double-phase layer consists of an exterior phase of FeB and interior phase of Fe<sub>2</sub>B, whereas the morphology of the boride layer is a

saw-tooth structure as shown in Figure 2.1. The saw-tooth structure helps improving the mechanical adherence at the  $\text{Fe}_2\text{B}$ /substrate interfaces.

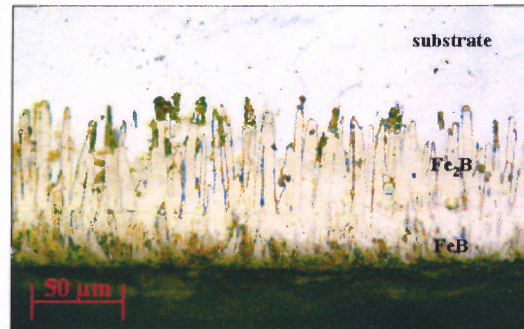


**Figure 2.1** The saw-tooth structure of boride layers with exterior layer  $\text{FeB}$  and interior layer  $\text{Fe}_2\text{B}$  of AISI 1018.

Because  $\text{FeB}$  phase is more brittle than  $\text{Fe}_2\text{B}$  phase, the formation of  $\text{Fe}_2\text{B}$  phase is expectedly preferred than that of  $\text{FeB}$  phase. In addition, it is observed that  $\text{Fe}_2\text{B}$  forms a surface under the high compressive stress, while  $\text{FeB}$  forms a surface under the high tensile stress. However, the boronizing process avoids having the coincidence of  $\text{Fe}_2\text{B}$  and  $\text{FeB}$  phases, which causes to the crack formation at the  $\text{FeB}/\text{Fe}_2\text{B}$  interface of double-phase layer. The crack formation leads to the spalling and even the separation of double-phase layer under the applied mechanical strain or the thermal/mechanical shock. Fortunately, the annealing process can decrease the occurrence of  $\text{FeB}$  phase after boronizing treatment <sup>[1]</sup>.

The characteristics of the  $\text{Fe}_2\text{B}$  phase include <sup>[34]</sup>:

- Composition with 8.83 wt% boron
- Body-centered tetragonal crystal structure ( $a=5.078\text{\AA}$ ,  $c=4.249\text{\AA}$ )
- Density of  $7.43\text{ g/cm}^3$
- Microhardness of about 18-20 GPa



- Young's modulus of 285-295 GPa
- Thermal expansion coefficient of  $7.65 \times 10^{-6} / ^\circ\text{C}$  in the range 200-600 °C, and  $9.2 \times 10^{-6} / ^\circ\text{C}$  in the range 100-800 °C

The characteristics of the FeB phase include <sup>[34]</sup>:

- Composition with 16.23 wt% boron
- Orthorhombic crystal structure ( $a=4.053 \text{ \AA}$ ,  $b=5.495 \text{ \AA}$ ,  $c=2.946 \text{ \AA}$ )
- Density of  $6.75 \text{ g/cm}^3$
- Microhardness of about 19-21 GPa
- Young's modulus of 590 GPa
- Thermal expansion coefficient of  $23 \times 10^{-6} / ^\circ\text{C}$  in the range 200-600 °C

### 2.3 Boronizing of Nonferrous Materials

Refractory metals, titanium, nickel, cobalt and their alloys can be boronized by using special techniques such as gas and plasma boronizing, instead of conventional boronizing techniques. Since the salt bath and conventional powder boronizing techniques are inapplicable for titanium and refractory metals because of the oxidation on the substrate and the corrosion from the activator that cause the porosity in the boride layer <sup>[33]</sup>. Therefore, the heat treatment for refractory and titanium metals is required to be operated under high vacuum and high purity argon atmosphere, or with the gas ( $\text{H}_2\text{-BCl}_3$ ) boronizing technique.

For the refractory metal and titanium, the process is prepared at the temperature above 1000 °C for ~10-15 hr <sup>[33]</sup>. The resulting boride layer is about 50  $\mu\text{m}$  thick with high microhardness values (Table 2.1). However, the boride layer of tantalum, tungsten,

niobium, molybdenum, and nickel metal does not show the strong saw-tooth structure as seen in titanium and cobalt metal <sup>[34]</sup>. Furthermore, the saw-tooth structure in nonferrous materials is not manifestly when compared to that in ferrous materials (low/medium carbon alloy).

## 2.4 The Mechanism of Boronizing Process

The boronizing process consists of two reactions:

1. The initial stage takes place between boron medium and component surface. The nuclei are formed as the function of boronizing temperature and time and are followed by the growth of boride layer <sup>[34]</sup>. In case of ferrous materials <sup>[35-36]</sup>, Fe<sub>2</sub>B nuclei are first formed and grow a thin boride layer at the defect points of the metal surface, macrodefects (surface roughness, scratches, etc.) and microdefects (grain boundaries, dislocation, etc.). If the active boron medium is excess, the rich boron product phase, such as FeB, will form and grow on the Fe<sub>2</sub>B phase.

2. The second stage is a diffusion-controlled process, which the thickness of boride layer is formed under a parabolic time law:

$$x^2 = kt$$

where  $x$  as the thickness of the boride layer,  $k$  as a constant depending on the temperature, and  $t$  as the boronizing time <sup>[34]</sup>. In case of ferrous materials, boron atoms prefer to diffuse in the [001] crystallographic direction and form the body-centered tetragonal lattice of Fe<sub>2</sub>B to achieve the maximum atomic density along this direction <sup>[35-</sup>

<sup>36]</sup>. The growth of  $\text{Fe}_2\text{B}$  is columnar aggregates of crystals, which exhibits the saw-tooth morphology. For the double phase, the columnar growth of  $\text{FeB}$  prefers to grow in the  $[002]$  crystallographic direction and the saw-tooth structure of  $\text{FeB}$  is lower than that of  $\text{Fe}_2\text{B}$ .

## 2.5 Effects of Alloying Elements

The prominent saw-tooth structure of boride layer is well observed in pure iron, unalloyed low-carbon steel, and low alloy steels. When the alloying elements and/or carbon contents in the substrate steel are increased, the thickness of the boride layer is reduced. In addition, the smooth interface may be observed instead of the saw-tooth structure illustrated in Figures 2.2 and 2.3. Another effect of alloying elements (except nickel, cobalt, and manganese), which retard the boron diffusion into the substrate, is to increase the proportion of  $\text{FeB}$  constitution <sup>[33]</sup>. For example in boronized stainless steel, the consequence of alloying elements leads to the thin smooth interface with almost 100%  $\text{FeB}$  formation of boride layer.

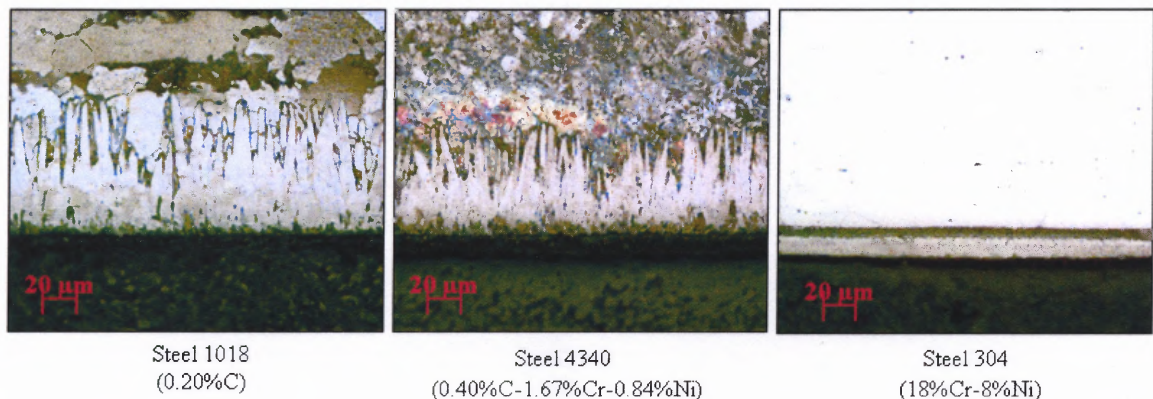


**Figure 2.2** The effect of steel composition on the morphology and thickness of the boride layer.

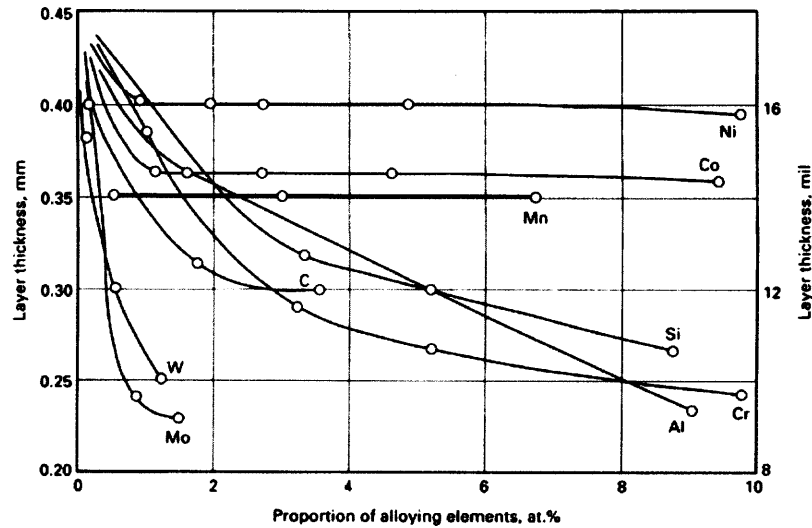


**Figure 2.3** The effect of percent alloying elements on the boride layer thickness <sup>[2]</sup>.

**Carbon, Silicon, and Aluminum** is insoluble in the boride layer. During the boronizing, the boride layer will drive carbon and silicon away from the surface to the substrate matrix and forms the precipitation of iron silicoboride ( $\text{FeSi}_{0.4}\text{B}_{0.6}$  or  $\text{FeSiB}_2$ ) and iron carboboride ( $\text{Fe}_{23}(\text{B,C})_6$  and  $\text{Fe}_3(\text{B,C})$ ) beneath and/or between the boride saw-teeth structure. The contents of silicon and aluminium (larger than 0.8%) underneath the boride layer can form a soft ferrite phase, which has a low load-carrying capacity <sup>[37]</sup>. Under the high surface pressure, the failure can occur due to the hard boride layer penetrating into this soft ferrite region.

**Nickel** will restrict the solubility of boron atoms in iron by diffusing into the boride layer and by precipitating  $\text{Ni}_3\text{B}$  from the boride layer at the  $\text{Fe}_2\text{B}$ /substrate interface. The result is the reduction of boride-layer thickness and saw-tooth structure. Although nickel may slightly reduce the microhardness value of the boride layer, nickel helps impeding the formation of  $\text{FeB}$  <sup>[37]</sup>.

**Chromium** is a modifier for the structure and properties of boride layer. The solubility of chromium in the  $\text{Fe}_2\text{B}$  phase causes the replacement from iron to chromium and forms  $(\text{Fe,Cr})\text{B}$  and  $(\text{Fe,Cr})_2\text{B}$  on the surface. The incorporation of chromium may increase the microhardness of boride layer but it causes boron to diffuse along the grain boundaries. The diffusion leads to the decreasing of boride layer thickness and the increasing of the smooth boride layer/substrate interface <sup>[37]</sup>. Chromium also promotes the formation of rich boron product phase, such as  $\text{FeB}$ , to the boride layer.

**Manganese, Tungsten, Molybdenum, and vanadium** are typically to reduce the boride thickness and flatten out the saw-tooth morphology.

## 2.6 Advantages and Disadvantages of Boronizing

### Advantages:

- The boronized steels can provide the extremely high hardness, compared with other treatments and other hard materials as listed in Table 2.2 and Figure 2.4.
- The combination of a high surface hardness and a low surface coefficient of friction in boronized steel provides the outstanding of wear mechanisms, including adhesion, tribooxidation, abrasion, and surface fatigue.
- The surface hardness of boronized steel can retain at high temperature.
- The process can be applied to a variety of metals and alloys.
- Boronized surfaces of ferrous materials have a high corrosion-erosion resistance in dilute acid and alkali media and are available in the industrial applications.
- Boronized surfaces have a moderate oxidation resistance (up to 850 °C or 1550 °F).

- Boronized surfaces are resistant to the attacks by molten metals.
- The boronized steels can increase the fatigue life and the service performance under the normal application and oxidation or corrosion environment.

**Disadvantages:**

- The technique is inflexible and rather labor-intensive. Therefore, the process is less cost-effective than other thermo-chemical treatments.
- The boride thickness cannot be well controlled because the thickness growth depends on the substrate composition and the consistency of boronized powder composition.
- The formation of boride layer increases the dimension of the base metal. The removal of the boride layer in order to meet the closer tolerance requirements is required to use the diamond lapping, since the conventional grinding causes the fracture of the layer.

**Table 2.2** The Surface Hardness of Boronized Steels Compares to Other Treatments and Hard Materials [2]

Material	Microhardness kg/mm <sup>2</sup> or HV
Boride mild steel	1600
Borided AISI H13 die steel	1800
Borided AISI A2 steel	1900
Quenched steel	900
Hardened and tempered H13 die steel	540-600
Hardened and tempered A2 die steel	630-700
High-speed steel BM42	900-910
Nitrided steels	650-1700
Carburized low-alloy steels	650-950
Hard chromium plating	1000-1200
Cemented carbides, WC + Co	1160-1820 (30 kg)
Al <sub>2</sub> O <sub>3</sub> + ZrO <sub>2</sub> ceramic	1483(30 kg)
Al <sub>2</sub> O <sub>3</sub> + TiC + ZrO <sub>2</sub> ceramic	1738 (30 kg)
Sialon ceramic	1569 (30 kg)
TiN	2000
TiC	3500
SiC	4000
B <sub>4</sub> C	5000
Diamond	>10,000

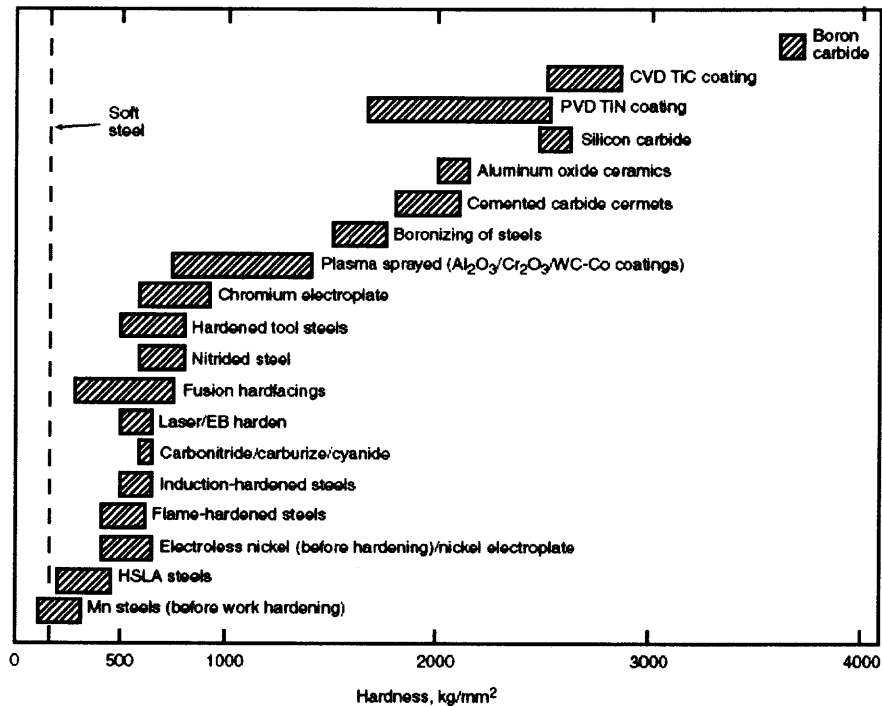


**Figure 2.4** The hardness value for various materials and surface treatments [38].

## 2.7 Application of Boronized Products

The conclusive boronized parts have been widely used in a variety of industrial applications as shown in Table 2.3.

**Table 2.3** The Application of Boronized Ferrous Materials <sup>[2]</sup>

Substrate material			Application
AISI	BSI	DIN	
		St37	Bushes, bolts, nozzles, conveyer tubes, base plates, runners, blades, thread guides
1020	...	C15 (Ck15)	Gear drives, pump shafts
1043	...	C45	Pins, guide rings, grinding disks, bolts
		St50-1	Casting inserts, nozzles, handles
1138	...	45S20	Shaft protection sleeves, mandrels
1042	...	Ck45	Swirl elements, nozzles (for oil bumpers), rollers, bolts, gate plates
		C45W3	Gate plates
W1	...	C60W3	Clamping chucks, guide bars
D3	...	X210Cr12	Bushes, press tools, plates, mandrels, punches, dies
C2	...	115CrV3	Drawing dies, ejectors, guides, insert pins
		40CrMnMo7	Gate plates, bending dies
H11	BH11	X38CrMoV51	Plungers, injection cylinders, spruce
H13	...	X40CrMoV51	Orifices, ingot molds, upper and lower dies and matrices for hot forming, disks
H10	...	X32CrMoV33	Injection molding dies, fillers, upper and lower dies and matrices for hot forming
D2	...	X155CrVMo121	Threaded rollers, shaping and pressing rollers, pressing dies and matrices
		105WCr6	Engraving rollers
D6	...	X210CrW12	Straightening rollers
S1	~BS1	60WCrV7	Press and drawing matrices, mandrels, liners, dies, necking rings
D2		X165CrVMo12	Drawing dies, rollers for cold mills
L6	BS224	56NiCrMoV7	Extrusion dies, bolts, casting inserts, forging dies, drop forges
		X45NiCrMo4	Embossing dies, pressure pad and dies
02	~BO2	90MnCrV8	Molds, bending dies, press tools, engraving rollers, bushes, drawing dies, guide bars, disks, piercing punches
E52100	...	100Cr6	Balls, rollers, guide bars, guides
		Ni36	Parts for nonferrous metal casting equipment
		X50CrMnNiV229	Parts for unmagnetizable tools (heat treatable)
4140	708A42 (En19C)	42CrMo4	Press tools and dies, extruder screws, rollers, extruder barrels, non-return valves
4150	~708A42 (CDS-15)	50CrMo4	Nozzle base plates
4317	...	17CrNiMo6	Bevel gears, screw and wheel gears, shafts, chain components
5115	...	16MnCr5	Helical gear wheels, guide bars, guiding columns
6152	...	50CrV4	Thrust plates, clamping devices, valve springs, spring contacts
302	302S25 (EN58A)	XI2CrNi188	Screw cases, bushes
316	~316S16 (EN58J)	X5CrNiMo1810	Perforated or slotted hole screens, parts for the textile and rubber industries
		G-X10CrNiMo189	Valve plugs, parts for the textile and chemical industries
410	410S21 (En56A)	X10Cr13	Valve components, fittings
420	~420S45 (EN56D)	X40Cr13	Valve components, plunger rods, fittings, guides, parts for chemical plants
		X35CrMo17	Shafts, spindles, valves
Gray and ductile cast iron			Parts for textile machinery, mandrels, molds, sleeves



## CHAPTER 3

### BORONIZING PROCEDURE

#### 3.1 Pack Boronizing

The pack boronizing or solid state boronizing technique is the most widely favored technique due to the simplicity and economy. The process involves the embedding of the metals/alloys into the boronizing powder mixture that consists of three substance groups [33].

- Boron source: Boron carbide ( $B_4C$ ), ferroboration, and amorphous boron
- Activator:  $NaBF_4$ ,  $KBF_4$ ,  $(NH_4)_3BF_4$ ,  $NH_4Cl$ ,  $Na_2CO_3$ ,  $BaF_2$ , and  $Na_2B_4O_7$
- Diluent:  $SiC$ ,  $Al_2O_3$

In the heat-resistant container, the well-cleaned and smooth metals/alloys are packed in the boronizing powder mixture with 10-20 mm thick and 50-100 mm deep, and covered by a container lid. The heat treatment is processed in the furnace. After reaching the boronizing temperature and time, the container is then removed from the furnace and allowed to cool down at room temperature. To avoid the adverse effect of oxygen on boronizing, the boronizing treatment should be performed under the protective-gas atmosphere, such as Ar,  $N_2$ ,  $H_2$ , or mixture of Ar- $N_2$ - $H_2$ . The protective-gas must be maintained after boronizing until the process is cooled down to 300 °C (570 °F) [1].

Using the above procedure, the boronizing powder mixture can be reused about 5-6 times by blending in 20-50% with the new powder mixture [2].

### 3.2 Paste Boronizing

The paste boronizing technique is practical for the large components or partially or selectively required part of components. The boronizing paste consists of 55%B<sub>4</sub>C (grain size 200-240μm) and 45%cryolite (Na<sub>3</sub>AlF<sub>6</sub>)<sup>[30]</sup>, or the traditional boronizing powder mixture (B<sub>4</sub>C-SiC-KBF<sub>4</sub>) with the binder, such as nitrocellulose/ butyl acetate, methylcellulose, or hydrolyzed ethyl silicate<sup>[33]</sup>. The method to apply the paste can be dipping, brushing, or spraying with the thick layer about 1-2 mm and is processed under the protective-gas atmosphere. After the heat treatment, the boronizing paste is removed by blast cleaning, brushing or washing.

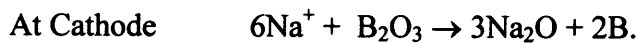
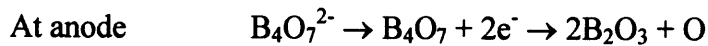
### 3.3 Liquid Boronizing

The liquid boronizing or salt bath boronizing technique is performed in the borax-based salt melts (Na<sub>2</sub>B<sub>4</sub>O<sub>7</sub>) with and without electrolysis at the temperature above 900 °C<sup>[33]</sup>. The technique is suitable for the complex body. The component must resist to the thermal shock of immersion and removal from the bath to prevent the component deformation and cracking. After treatment, the excess melting salt must be removed from the component, causes the high cost and time consuming. The maintenance cost is also high because the process requires the salt recharging for the appropriate viscosity to prolong the boronizing reaction. The corrosive fume from the reaction creates another problem to the technique.

- **Electroless liquid boronizing:** The common salt bath is 30-70% Borax-B<sub>4</sub>C and the reaction is enhanced by replacing 20% B<sub>4</sub>C with ferroaluminium because of the

effective reductant. For the nickel alloy, the bath is composed of 75%wt  $\text{KBF}_4$  - 25%wt  $\text{KF}$ , operating at temperature below  $670\text{ }^\circ\text{C}$ .

- **Electrolytic liquid boronizing:** The component is attached to a cathode, while the graphite is acted as an anode. Both of them are immersed in the molten borax at  $940\text{ }^\circ\text{C}$  and the current ( $0.15\text{A}/\text{cm}^2$ ) is passed to them. At the liquid state, Borax is decomposed to sodium ions ( $\text{Na}^+$ ) and tetraborate ( $\text{B}_4\text{O}_7^{2-}$ ). The reaction is as followed:



### 3.4 Gas Boronizing

The gas boronizing technique is a diffusion process of some gas media, such as diborane ( $\text{B}_2\text{H}_6$ ) or boron chloride ( $\text{BCl}_3$ ). This method is unavailable for the industry concerned by the toxic and the explosion of gas media. The  $\text{BCl}_3\text{-H}_2$  gas mixture has previously been attempted to boronize the steel, but the high concentration of  $\text{BCl}_3$  causes the corrosion on the substrate and results the poor adherent layers. To improve the technique, the dilute (1:15)  $\text{BCl}_3\text{-H}_2$  gas mixture is commonly used at  $700\text{-}900\text{ }^\circ\text{C}$  and under the pressure of about  $67\text{ kPa}$  [39]. Moreover, the replacing of a carrier-reductant gas of 75% $\text{N}_2$  and 25% $\text{H}_2$ , rather  $\text{H}_2$ , can reduce the  $\text{BCl}_3$  concentration. As a result, it avoids  $\text{FeCl}_3$  (corrosion) and diminishes the  $\text{FeB}$  formation. As well, this process can be used with titanium and its alloys.

### 3.5 Plasma Boronizing

The plasma boronizing technique is not yet available in the commercial application because of the same problems as occurred in the gas boronizing technique. The gas mixtures of  $B_2H_6-H_2$  and  $BCl_3-H_2-Ar$  are used in this technique. Additionally, the  $BCl_3-H_2-Ar$  gas mixture exhibits good features of controlling an amount of  $BCl_3$  concentration. The resulting features reduce the discharge voltage and increase the microhardness of the boride layer <sup>[40]</sup>. Despite the porosity of double-phase boride layer is observed, increasing the  $BCl_3$  concentration can minimize it. This technique is widely applied to the refractory metals because of the high-efficient deposition of the boride layer, which is higher than that of the pack boronizing technique. By this technique, the process can be operated at the low temperature  $\sim 600$  °C (1100 °F) and in the short time, which helps saving in energy and gas consumption. The conventional pack boronizing technique, however, cannot operate at such low temperature.

### 3.6 Fluidized Bed Boronizing

The fluidized bed boronizing technique is a recent innovation of boronizing. The bed materials, coarse-grained silicon carbide and boronizing powder mixture, are served as a faster heat-transfer medium through which an oxygen-free gas ( $N_2-H_2$ ) flows. The high heating rate and high flowing rate provide the rapid boronizing, meaning the shorter operation time. Because of the temperature uniformity, the process can also produce the reproducibility, good tolerances, and uniform finishing mass-products. Finally, this technique achieves the low operating cost for the mass production of boronized parts. However, the major disadvantage is the exhaust gases (fluorine compounds) that must be

completely eliminated by using the  $\text{CaCO}_3$  absorber to avoid the environmental problems.

### 3.7 Multi-component Boronizing

The multi-component boronizing technique is the process that combines the diffusion of boron and one or more metallic element(s), including aluminium, chromium, vanadium, and silicon, into the substrate surface. Some multi-component boronizing systems are illustrated in Table 3.1. The multi-component boronizing can be classified into three types<sup>[33]</sup>:

- Type 1: simultaneous boronizing and metallizing
- Type 2: boronizing followed by metallizing
- Type 3: metallizing followed by boronizing

**Table 3.1** The Multi-Component Boronizing

Reference	Multi-component boronizing technique	Media type	Media composition, wt%	Process steps investigated*	Substrate(s) treated	Temperature, °C (°F)
41	Boroaluminizing	Electrolytic salt bath	3-20% $\text{Al}_2\text{O}_3$ in borax	S	Plain carbon steels	900 (1650)
42	Boroaluminizing	Pack	(A) 84% $\text{B}_4\text{C}$ + 16% borax (B) 97% ferroaluminium + 3% $\text{NH}_4\text{Cl}$	S B-Al Al-B	Plain carbon steels	1050 (1920)
43	Borochromizing	Pack	(A) 5% $\text{B}_4\text{C}$ + 5% $\text{KBF}_4$ + 90% SiC (Ekabor II) (B) 78% ferrochrome + 20% $\text{Al}_2\text{O}_3$ + 2% $\text{NH}_4\text{Cl}$	S B-Cr Cr-B	Plain carbon steels	Borided at 900 (1650) Chromized at 1000 (1830)
43	Borosiliconizing	Pack	(A) 5% $\text{B}_4\text{C}$ + 5% $\text{KBF}_4$ + 90% SiC (Ekabor II) (B) 100% Si	B-Si Si-B	0.4% C steel	900-1000 (1650-1830)
43	Borovanadizing	Pack	(A) 5% $\text{B}_4\text{C}$ + 5% $\text{KBF}_4$ + 90% SiC (Ekabor II) (B) 60% ferrovanadium + 37% $\text{Al}_2\text{O}_3$ + 3% $\text{NH}_4\text{Cl}$	B-V	1.0% C steel	Borided at 900 (1650) Vanadized at 1000 (1830)

\* S = simultaneous boronizing and metallizing.

B-Al = boronized and then aluminized, Al-B= aluminized and then boronized.

The attracting result from this process is an improvement of mechanical properties and oxidation resistance as stated below:

- Boroaluminizing – the compact layer provides good wear and corrosion resistance, especially in humid environments
- Borosiliconizing – the FeSi is formed on the boride-layer surface that increases the corrosion-fatigue strength of component.
- Borochromizing – this treatment provides the better oxidation resistance than boroaluminizing, gives the uniform layer, improves the wear resistance, and increases the corrosion-fatigue strength.
- Borovanadized and borochromvanadized – the layer will have ductility with a high microhardness (>3000HV at 15g load), which helps reducing the spalling under the impact loading condition.

## **CHAPTER 4**

### **PROPERTIES OF BORONIZED STEELS**

After boronizing, steels will have the desirable properties on the surface, including the increasing wear resistance, corrosion resistance, and 3-10 times increasing service life.

#### **4.1 Toughness**

The boride layer provides the good bonding with the base metal, which can ensure that under load, the flaking or the peeling will not happen. However, the toughness of the boronized steel relies on its boride layer thickness, cross-section area, and mechanical properties. In the bending test, the boronized sample with the boride-layer thickness of 150-200  $\mu\text{m}$  has 4% elongation without cracking <sup>[1]</sup>.

#### **4.2 Adhesion Resistance**

The boronized surfaces show neither accretion nor wear of material as well as having hardly any tendency to cold-weld <sup>[37]</sup>. Consequently, this property is used in the cold-metal working (chipless shaping) as a tool to form the metals. Without the non-lubricant, the boronized layers do not have an appreciable change at 300 °C in order to protect the environment by reducing the lubricant.

#### **4.3 Abrasive Wear Resistance**

High microhardness provides high wear resistance. Some resulting properties of boronized steels are shown in Figures 4.1 and 4.2.

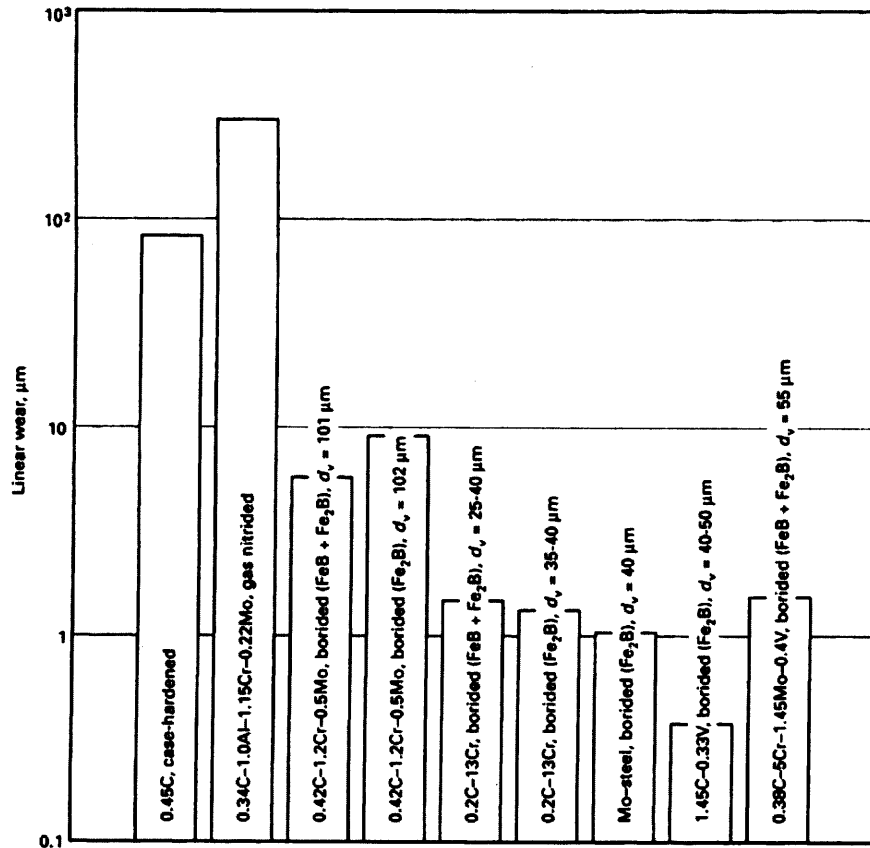


**Figure 4.1** The effect of steel composition (nominal values in wt %) on wear resistance under abrasive wear ( $d_v$  = thickness of the boride layer); Test conditions: DP-U grinding tester, SiC paper 220, testing time 6 minutes [2].

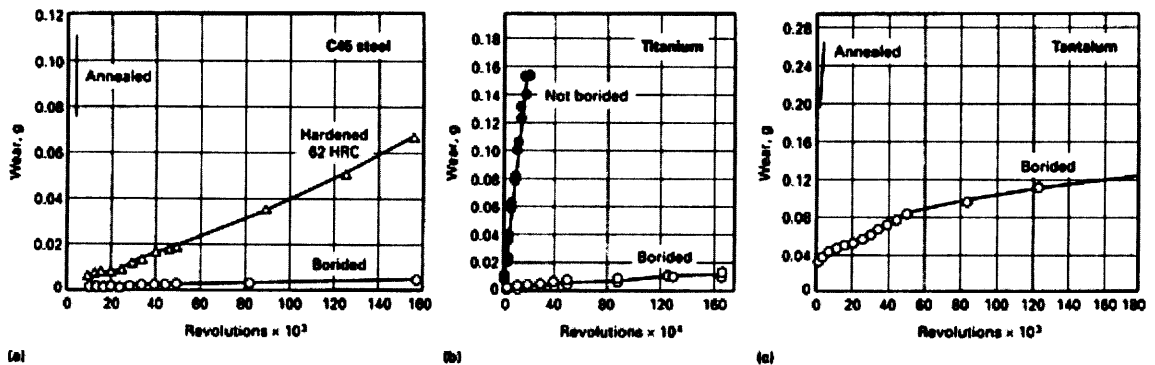


**Figure 4.2** The comparison of wear resistance between boronized steels and non-boronized steel [2].



#### 4.4 Corrosion Resistance in Acids

Boronized carbon and alloy steel have the increasing corrosion resistance in HCl, H<sub>2</sub>SO<sub>4</sub>, and H<sub>3</sub>PO<sub>4</sub>. The boronized austenitic stainless steel improves the corrosion resistance in HCl as shown in Figure 4.3.

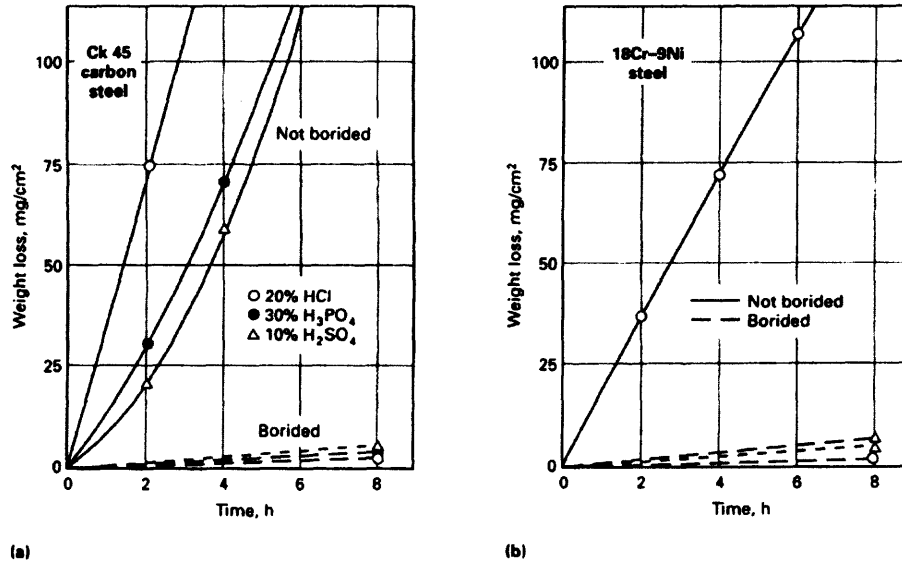


**Figure 4.3** The comparison of corrosion resistance between boronized steels and non-boronized steels [2].

**CHAPTER 5**  
**EXPERIMENTAL PARTS**

**5.1 Description of Experiments**

The steel samples (AISI 1018, AISI 4340, and AISI 304) were chosen to boronize at 850 °C for four hours under the argon atmosphere. The boride layer of boronized steel samples was characterized in terms of phase identification, thickness, morphology, and microhardness. The corrosion resistances of both unboronized and boronized steel samples were observed as well as the oxidation resistance. The experimental flow chart was illustrated in Figure 5.1.

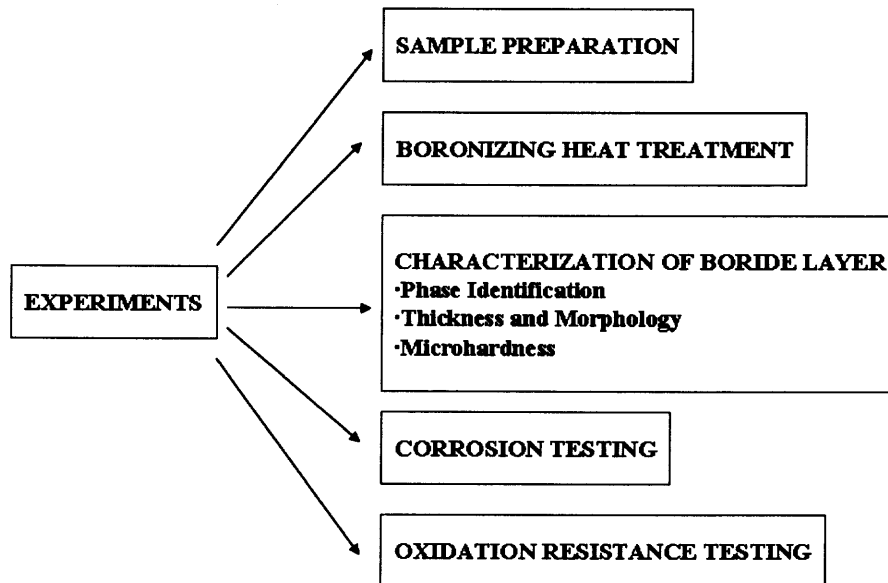


**Figure 5.1** The experimental description flow chart.

## 5.2 Experimental Procedures

The experimental procedures were described as below:

### 5.2.1 Sample Preparation

AISI 1018, AISI 4340, and AISI 304 samples were cut in the dimension of  $10 \times 10 \times 3$  mm,  $12 \times 12 \times 7$  mm, and  $12 \times 10 \times 6$  mm, respectively. The chemical composition of sample steels was shown in Table 5.1. Firstly, the samples were grinded with the 120, 220, 400, and 600-grit sand papers. The samples, then, were cleaned with acetone in the ultrasonic bath for 5-10 minutes and dried in the air.

**Table 5.1** The Chemical Composition of Steel Samples

Steel	Chemical Composition, %												
	C	Mn	P	S	Si	Cu	Ni	Cr	Mo	Al	V	Co	N
1018	0.200	0.720	0.008	0.008	0.016	-	-	-	-	0.065	-	-	-
4340	0.400	0.75	0.008	0.005	0.230	0.140	1.67	0.84	0.27	0.028	0.004	-	-
304	0.022	1.58	0.030	0.028	0.41	0.49	8.05	18.20	0.44	-	-	0.110	0.090

### 5.2.2 The Procedure of Boronizing Heat Treatment

The boronizing heat treatment procedures can be classified into three steps.

**5.2.2.1 The Preparation of Boronizing Powder Mixture.** The boronizing power mixture was prepared by mixing together 1% w/w  $\text{KBF}_4$  (potassium tetrafluoroborate, 99% min (assay), typically >99.5% (assay) of Alfa Aesar), 5% w/w  $\text{Al}_2\text{O}_3$  (aluminum oxide powder, 99.99%, 20-30 micron of Atlantic Equipment Engineers), and 94% w/w  $\text{B}_4\text{C}$  (boron carbide, 240 grit, technical grade of Electro Abrasives Corporation).  $\text{KBF}_4$  and  $\text{Al}_2\text{O}_3$  were first mixed in the mortar to break the powder cluster and followed by

gradually adding a small quantity of  $B_4C$  to prevent the segregation of  $KBF_4$  and  $Al_2O_3$  powder from  $B_4C$  into the gradients. After all substances were mixed in the mortar, the boronizing powder mixture was mixed again in the blender to be confident that the component was well homogeneous.

**5.2.2.2 The Packing of Boronizing Powder.** The boronizing power mixture was dried at  $250\text{ }^\circ\text{C}$  for two hours in the box furnace (ThermoLyne model 48015). The well-cleaned sample steels were embedded in the boronizing power mixture contained in inconel crucible. After the boronizing powder mixture was filled full in the crucible, the crucible should be tapped until the powder mixture was densely packed. It was to prevent the air trap among the powders. Sequentially, the crucible full-filled with powder mixture was degassed overnight (approximately 12 hours) in the desiccator that connected to the vacuum system.

**5.2.2.3 The Boronizing Heat Treatment.** The crucible containing the boronizing powder mixture and the embedded sample steels was dried for two hours at  $250\text{ }^\circ\text{C}$  in the furnace. After that, the crucible lid was covered tightly. Then, the furnace temperature was increased to  $850\text{ }^\circ\text{C}$  and was held for four hours in the argon atmosphere (Argon (99.999%) of SOS Gases) with the flow rate 60 psi. After reaching the required temperature and time, the furnace was cool down to  $300\text{ }^\circ\text{C}$  under the argon atmosphere and the furnace was switched off. When the furnace was cool down to the room temperature, the boronized sample steels were removed from the crucible and were cleaned with the methanol in the ultrasonic bath.

### 5.2.3 Characterization of Boride Layers

The boride layers were analyzed with three aspects as follows.

**5.2.3.1 Phase Identification.** The X-ray Diffraction Method (XRD) was used to investigate the unboronized and boronized sample steel phases of AISI 1018, AISI 4340, and AISI 304. XRD Philips (PW3040 MPD DY715) was used under the system condition as followed: the XRD wavelength utilized was Cu K- $\alpha$ 1 (1.5405980 Å) at 45 kV and 40 mA; the ½" divergence slit, ½" anti-scatter slit, and 15 cm mask were chosen to detect the XRD spectrum; the  $2\theta$  scan range was from 20-100° with step size of 0.020 and 2.70 times per step. The specimen phase was analyzed by using X'Pert high score software.

**5.2.3.2 Morphology and Thickness.** The outer surface of boronized sample steels was observed by using optical microscopy. The AxioTech Microscope of Carl Zeiss with 10x eyepiece lens and 20x, 50x, 100x objective lens was used to investigate with Differential Interference Contrast (DIC), Darkfield, and Brightfield methods. The resulting microstructure images have been taken by using the digital camera (Pixelink PL-A662).

The cross-sectional specimen was used to examine the thickness and morphology of the boride layers penetrating into the steel substrates. The boronized sample steels were mounted with the epoxy resin (EpoxyMount of Allied High Tech Products, Inc.) in the two-part mounting cups. The mixing ratio of part A (resin) and part B (hardener) was 100:30 by weight. After mounted, the specimens were placed in the desiccator and degassed under the vacuum system for 10 minutes. They were then left to cure overnight

at room temperature and thereafter were removed from the mounting cups and continued with the grinding and polishing procedures.

The grinding and polishing machine (MetPrep3 from Allied High Tech Products, Inc.) was deployed. The grinding and polishing procedures are demonstrated in the Table 5.2.

**Table 5.2** The Grinding and Polishing Procedure for the Steel Substrates

Step	1	2	3	4	5	6	7
<b>Abrasive Size</b>	180 grit	320 grit	600 grit	6 micron	3 micron	1 micron	0.05 micron
<b>Abrasive Type</b>	SiC	SiC	SiC	Diamond Lapping Film	Diamond Compound	Diamond Compound	Colloidal Silica Suspension
<b>Carrier</b>	Grinding Disc	Grinding Disc	Grinding Disc	Type B			
<b>Polishing Cloth</b>	N/A	N/A	N/A	N/A	Gold Label	Imperial	Chem-Pol
<b>Extender</b>	H <sub>2</sub> O	H <sub>2</sub> O	H <sub>2</sub> O	BlueLube	RedLube	RedLube	N/A
<b>Platen Speed</b>	150 RPM (CCW)	150 RPM (CCW)	150 RPM (CCW)	150 RPM (CCW)	150 RPM (CCW)	150 RPM (CCW)	150 RPM (CCW)
<b>Hard Pressure</b>	8 LB	8 LB	8 LB	8 LB	8 LB	8 LB	8 LB
<b>Time</b>	3 min	3 min	3 min	3 min	3 min	3 min	3 min

Note: The consumer products are supplied by Allied High Tech Products, Inc.

After grinded and polished, the specimens were cleaned with water in the ultrasonic bath until all substances remaining from the polishing procedure was completely eliminated. They were dried with the air blower. To observe the morphology and thickness of boride layers, the AISI 1018 and AISI 4340 specimens would be etched by the etching solution of 0.5g picric acid (98% picric acid of Aldrich), 12.5g sodium

hydroxide (>98%(assay) sodium hydroxide of Fluka), and 25ml distilled water at 35 – 40 °C for one minute, while AISI 304 specimens were etched in 3% nitric acid. After etching the specimens were washed with water in the ultrasonic bath. It should not have any etching solution left on the specimen surface because the etching solution caused the distortion of the image color.

After that, the morphology microstructure of boride layers was observed with the optical microscope and the microstructure images were taken. The thickness of the boride layer was measured by using AxioVision Software Version 4.1 of Carl Zeiss. The measurement of each saw-tooth structure depth was randomly examined. Subsequently, the distribution and average value of thickness depth were calculated by using the statistic operation.

**5.2.3.3 Microhardness.** The microhardness of boronized sample steels (AISI 1018, AISI 4340, and AISI 304) was determined at every boride-layer depth by using LM700 Microhardness Tester with the Vickers indenter of Leco. The relationship between the Vickers microhardness and the boride layer depth was observed.

#### **5.2.4 Corrosion Testing**

The corrosion resistances of unboronized and boronized sample steels (AISI 1018, AISI 4340, and AISI 304) were investigated by a continuous weighting method. The weight loss of the specimen was continuously detected as a function of time. The 5%, 10%, 15% w/w hydrochloric acid (HCl) were used as corrosive media. The setting equipment for this experiment was illustrated in Figure 5.2.

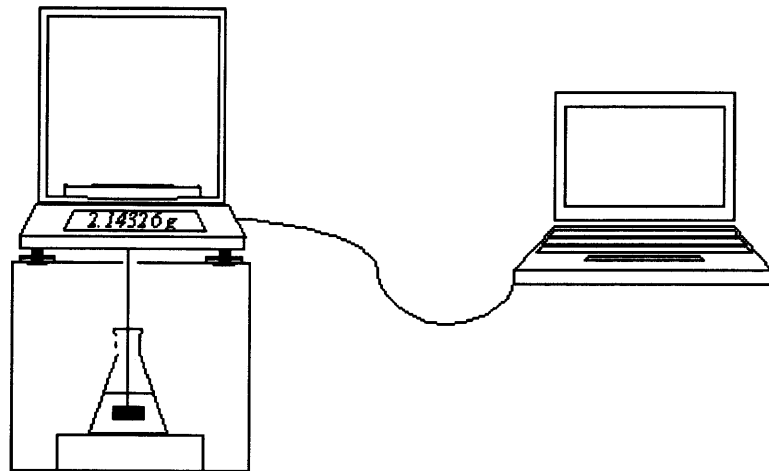


**Figure 5.2** The equipment setting for corrosion testing (continuous weighting method).

From Figure 5.2, the specimen was hung down from the balance (Analytical Balance GR-202 of A&D) with platinum wire and immersed in hydrochloric acid solution for 24 hours. The specimen weight was detected every 36 seconds and automatically stored in computer.

### **5.2.5 Oxidation Resistance Testing**

The oxidation resistance of unboronized and boronized steels (AISI 1018, AISI 4340, and AISI 304) was investigated at 600 °C for 2, 4, 6, 8, 10, 12 hours in the box furnace. The weighted specimen was placed inside the ceramic boat and then put into the furnace. Periodically every two hours, the specimen was removed from the furnace, cooled down at room temperature, and weighted. The weight gains of specimen were detected with respect to the soaking time.



## CHAPTER 6

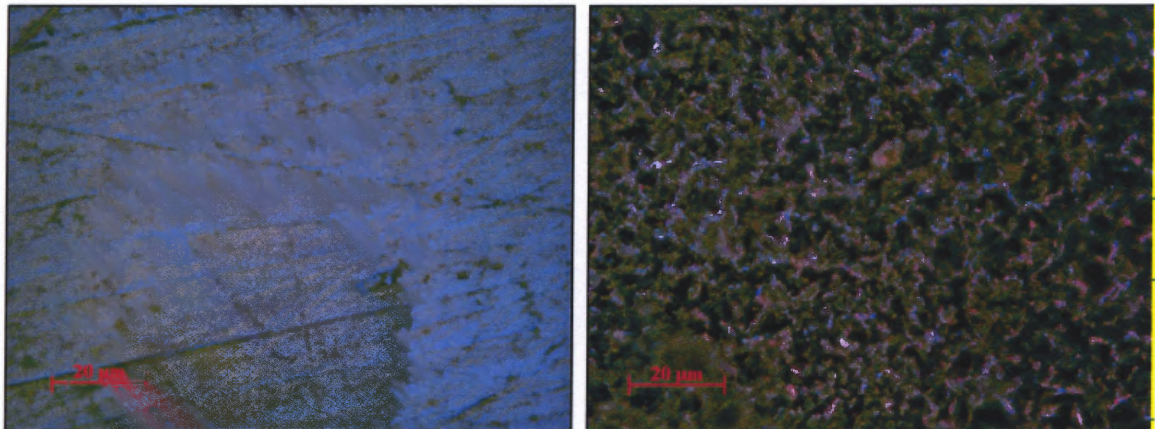
### RESULTS AND DISCUSSION

#### 6.1 Characteristics of Boride Layer

The analysis of boride layer shows the major characteristics into four aspects.

##### 6.1.1 Boride Surface

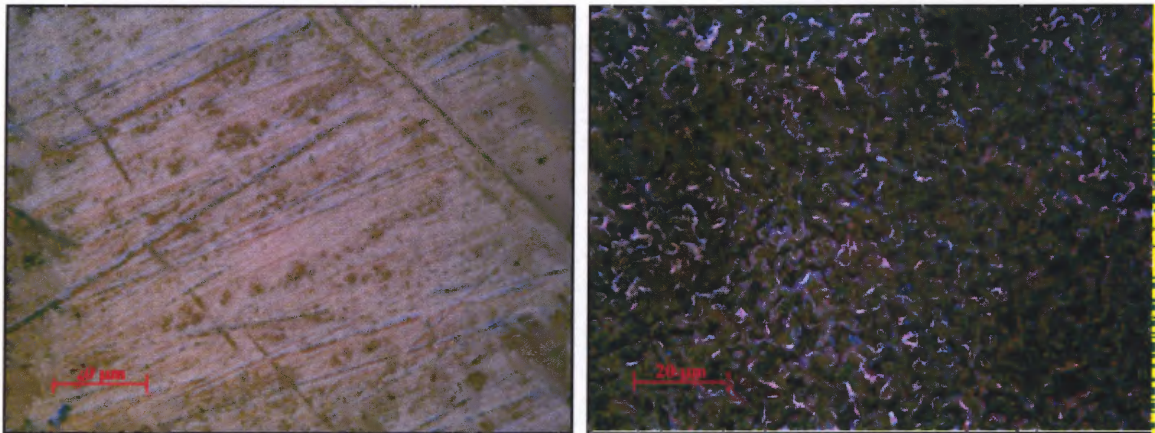
After the boronizing heat treatment, the sample surface was seen in dark grey color, which was a color of iron-boron compound ( $\text{FeB}$  and  $\text{Fe}_2\text{B}$ ). The image of specimen's surface before and after boronizing heat treatment was illustrated in Figures 6.1, 6.2 and 6.3. From these figures, it was indicated that the boride layer that occurred during the boronizing process increased the roughness of specimen's surface. Consequently, the roughness might be the problem of low specimen tolerance.



a) The specimen surface before boronizing

b) The specimen surface after boronizing

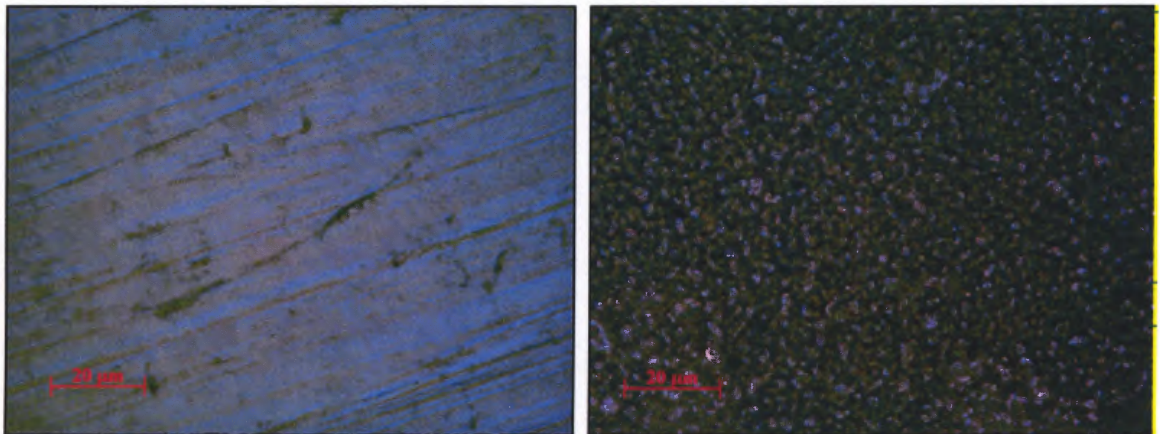
**Figure 6.1** The image of AISI 1018 specimen surface before and after boronizing.



a) The specimen surface before boronizing

b) The specimen surface after boronizing

**Figure 6.2** The image of AISI 4340 specimen surface before and after boronizing.



a) The specimen surface before boronizing

b) The specimen surface after boronizing

**Figure 6.3** The image of AISI 304 specimen surface before and after boronizing.

### 6.1.2 Phases Present in the Boride Layer

To detect the occurrence of boride-layer phases on the boronized specimen, the XRD pattern of unboronized specimen was used as a background phase. The different boride-layer phases deposited on the specimen surface after boronizing were shown in Table 6.1.

The XRD patterns of AISI 1018, AISI 4340, and AISI 304 were shown in Figures 6.4, 6.5, and 6.6, respectively.

**Table 6.1** The Boride Phase on the Specimen Surface

Steel	Phase Present
AISI 1018	Fe <sub>2</sub> B, FeB
AISI 4340	Fe <sub>2</sub> B, FeB
AISI 304	FeB

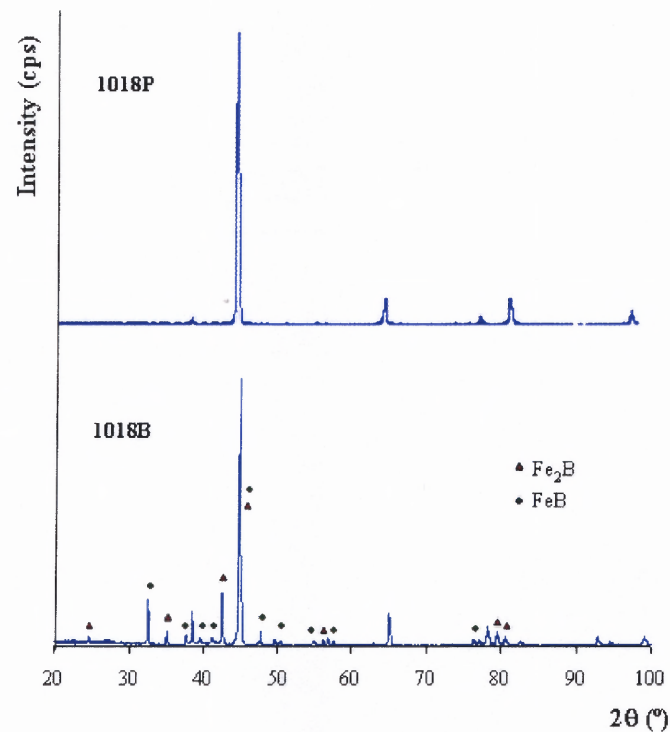


**Figure 6.4** The XRD pattern of AISI 1018 before and after boronizing (P-unboronized specimen, B-boronized specimen).

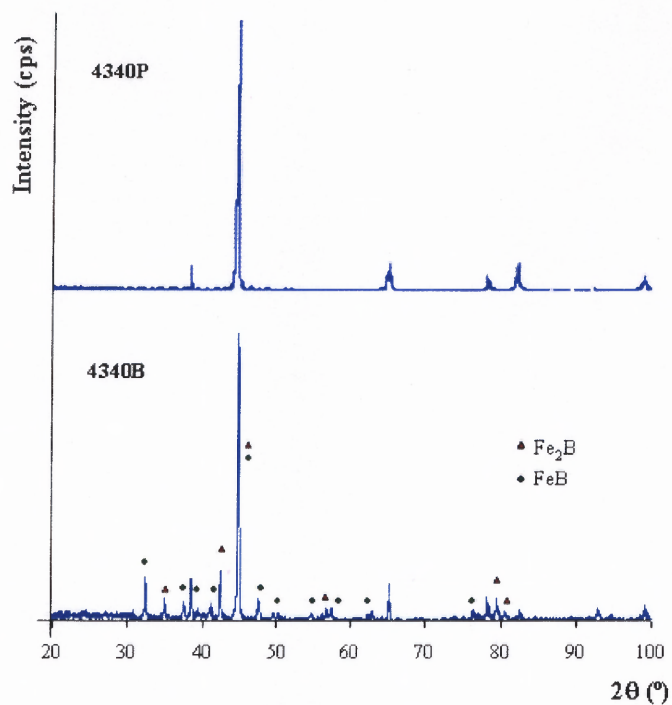


**Figure 6.5** The XRD pattern of AISI 4340 before and after boronizing (P-unboronized specimen, B-boronized specimen).

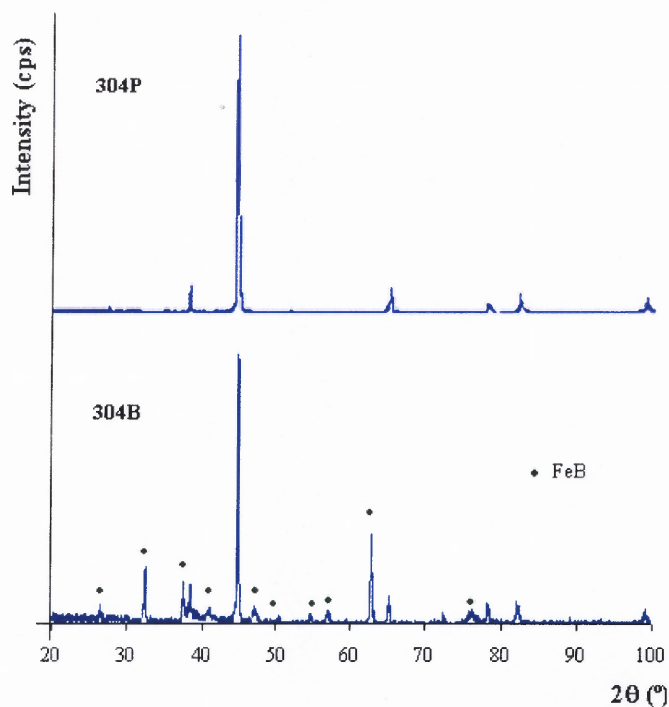


**Figure 6.6** The XRD pattern of AISI 304 before and after boronizing (P-unboronized specimen, B-boronized specimen).

### 6.1.3 The Morphology and Thickness of Boride Layer

The saw-tooth structure or the needle-like structure of boride layer penetrating into the substrate matrix was observed on the cross-sectional specimen. The microstructure image of inward  $\text{Fe}_2\text{B}$  phase and outward  $\text{FeB}$  phase was exhibited in brown color and blue color, respectively. The average boride-layer thickness of AISI 1018, AISI 4340, and AISI 304 was shown in Table 6.2. The distribution of the boride-layer thickness and the cross-sectional specimen morphology were also shown in Figures 6.7, 6.8, and 6.9.

**Table 6.2** The Boride-layer Thickness on Steel Substrate

Steel	Average Boride-layer Thickness ( $\mu\text{m}$ )
AISI 1018	75-76
AISI 4340	57-58
AISI 304	10-11

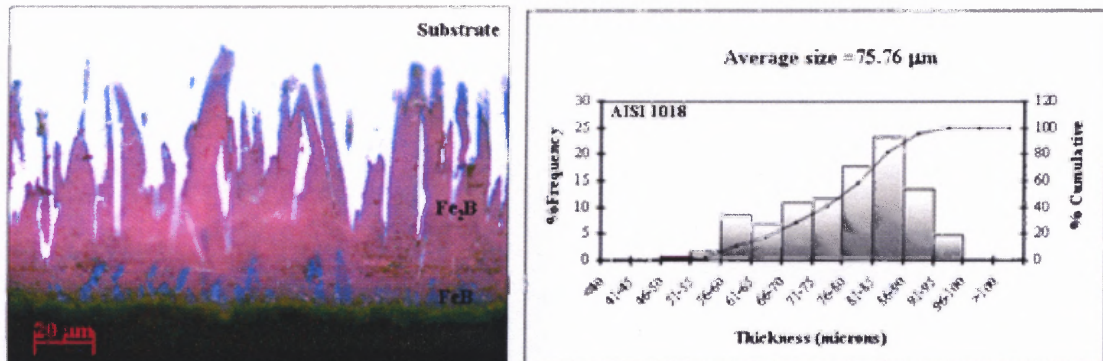


**Figure 6.7** The saw-tooth morphology and the distribution of the boride-layer thickness on AISI 1018.

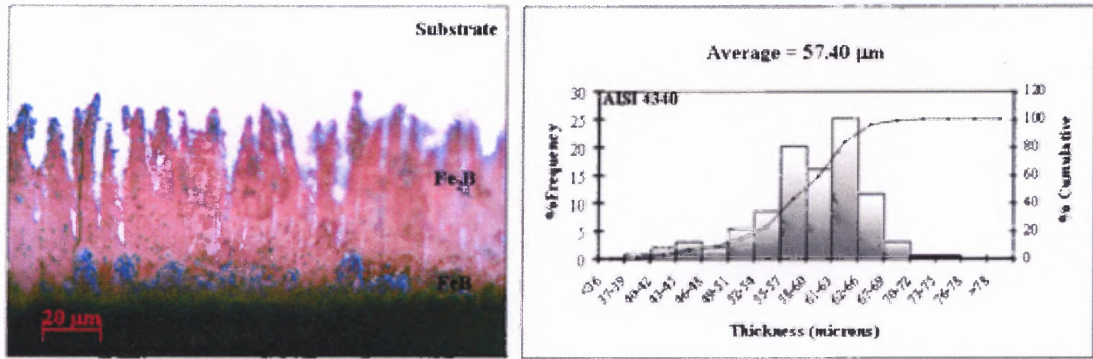


**Figure 6.8** The saw-tooth morphology and the distribution of the boride-layer thickness on AISI 4340.

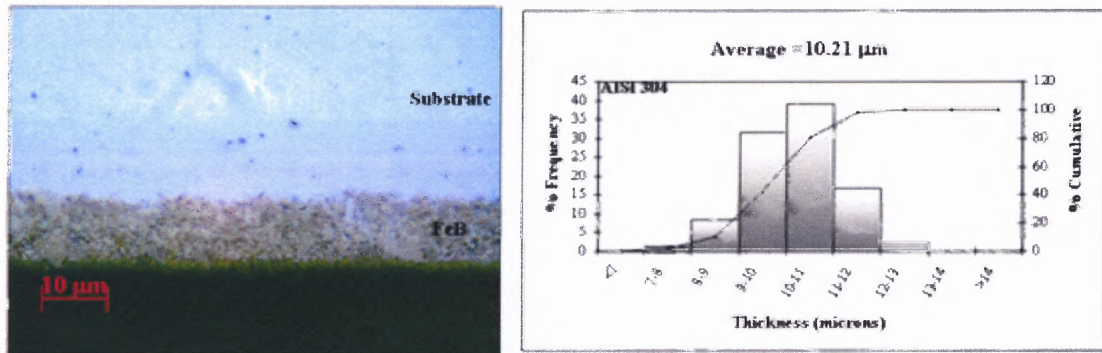


**Figure 6.9** The saw-tooth morphology and the distribution of the boride-layer thickness on AISI 304.

According to the chemical composition of steels in Table 5.1, it was seen that the boride-layer thickness was inverse to the alloying elements in the sample steels. The increasing of alloying elements caused the decreasing of boride-layer thickness. AISI 1018, plain carbon steel without alloying elements, demonstrated the saw-tooth structure with 75 – 76 µm in depth, while AISI 4340, high strength alloy steel, had more alloying elements than AISI 1018, showing the shorter saw-tooth structure of boride layer (57 - 58 µm). In case of AISI 304 (austenitic stainless steel), the narrow (10 -11 µm) and smooth boride layer was detected, which was the effect on the high quantities of chromium and nickel as alloying elements in AISI 304 steel substrate.

### 6.1.4 Microhardness

The microhardness of boride layer related to the amount of boron atoms that diffused into the substrate, in terms of the depth from the external surface. The fact that microhardness decreased as the depth from the surface increased was observed and illustrated in Figures 6.10, 6.11, and 6.12. Moreover, it was shown that the decline of microhardness became larger on going towards to the bulk of the substrate.

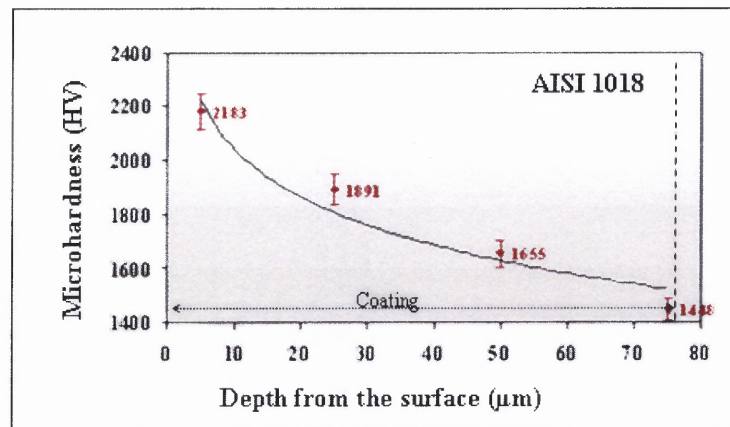


**Figure 6.10** The plot between the microhardness and the depth of boride layer in AISI 1018.

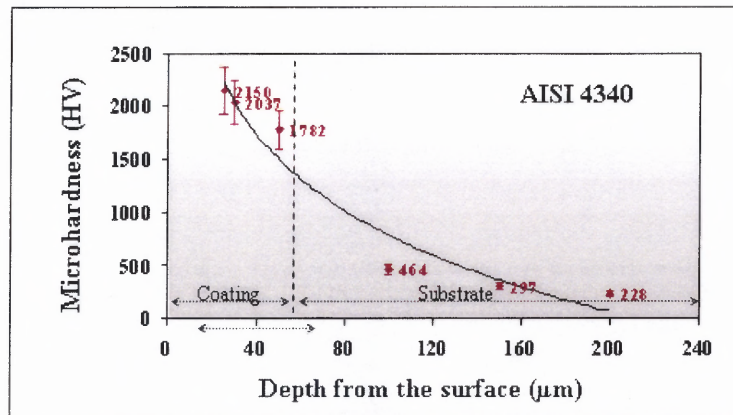


**Figure 6.11** The plot between the microhardness and the depth of boride layer in AISI 4340.

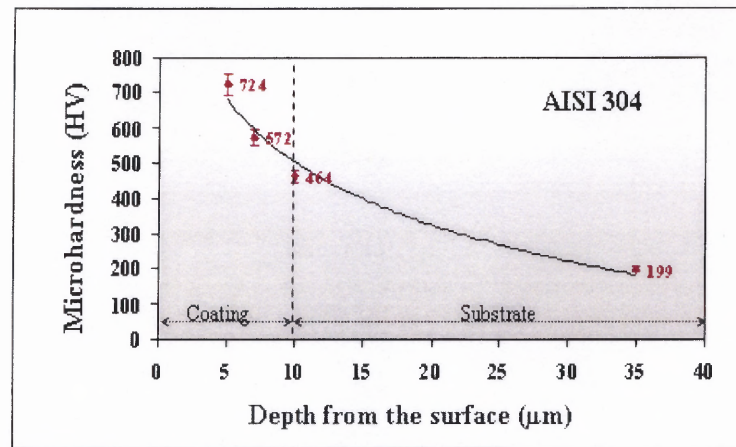


**Figure 6.12** The plot between the microhardness and the depth of boride layer in AISI 304.

## 6.2 Corrosion Testing

The corrosion resistance testing of boronized specimen was investigated in 5%, 10%, and 15% w/w hydrochloric acid, compared with that of unboronized specimen in 5% w/w hydrochloric acid. The unique technique (continuous weighting method) was used to investigate the results of corrosion resistance. For AISI 1018, the boronized sample was able to resist in 5% w/w hydrochloric acid but it could not protect the substrate from the acid corrosion in 10% and 15% w/w hydrochloric acid as shown in Figure 6.13. For AISI 4340, the boronized steel also enabled to protect the substrate from the corrosive media as shown in Figure 6.14. Especially, AISI 304, which usually could not persist in hydrochloric acid, was able to resist in hydrochloric acid as shown in Figure 6.14.



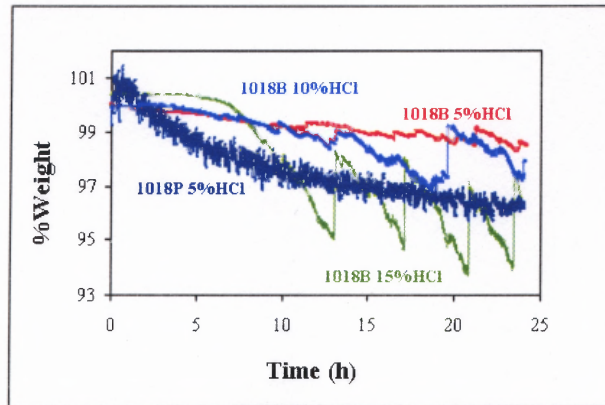


**Figure 6.13** The corrosion tests of unboronized and boronized specimen (AISI 1018) in HCl solution (B-boronized specimen, P-unboronized specimen).

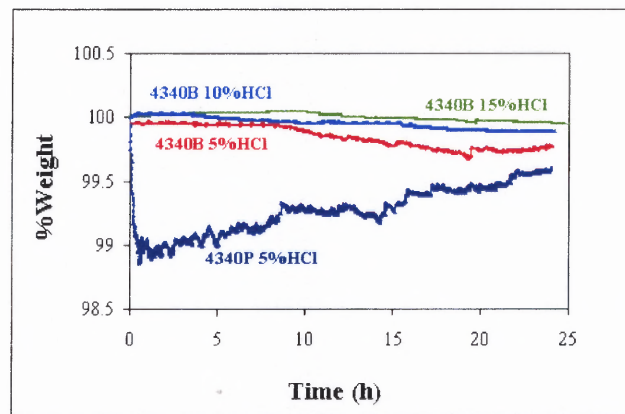


**Figure 6.14** The corrosion tests of unboronized and boronized specimen (AISI 4340) in HCl solution (B-boronized specimen, P-unboronized specimen).

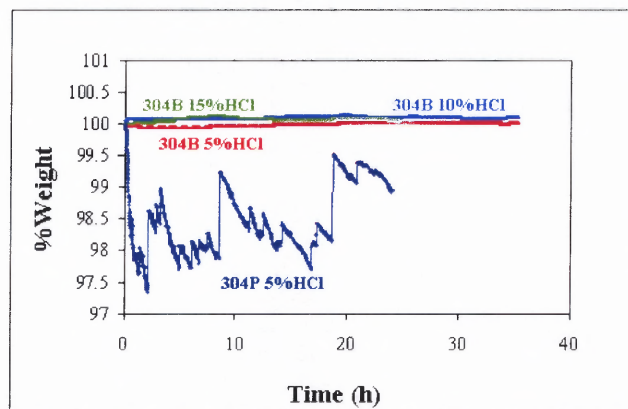


**Figure 6.15** The corrosion tests of unboronized and boronized specimen (AISI 304) in HCl solution (B-boronized specimen, P-unboronized specimen).

### 6.3 Oxidation Resistance Testing

The oxidation resistance of boronized and unboronized specimens was determined at 600 °C for 12 hours. In case of AISI 1018 illustrated in Figure 6.16, the experimental result showed that the oxidation resistance of boronized specimen was higher than that of unboronized specimen about three times. In case of AISI 4340 illustrated in Figure 6.17, during the beginning of experiment the oxidation resistance of boronized specimen was higher than that of unboronized specimen; however, after 8 hours the oxidation resistance of boronized specimen seemed constant while the unboronized specimen inclined continuously. In case of AISI 304 illustrated in Figure 6.18, the results showed the better oxidation resistance of boronized specimen than that of unboronized specimen.

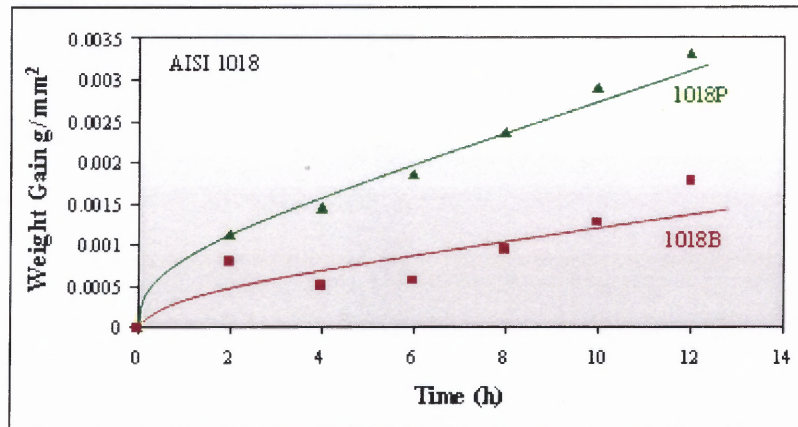


**Figure 6.16** The oxidation test of boronized and unboronized specimen (AISI 1018) at 600 °C for 12 hours (B-boronized specimen, P-unboronized specimen).

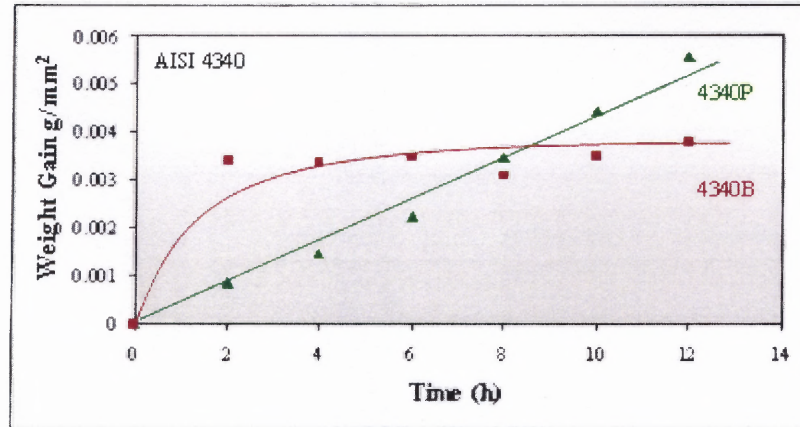


**Figure 6.17** The oxidation test of boronized and unboronized specimen (AISI 4340) at 600 °C for 12 hours (B-boronized specimen, P-unboronized specimen).

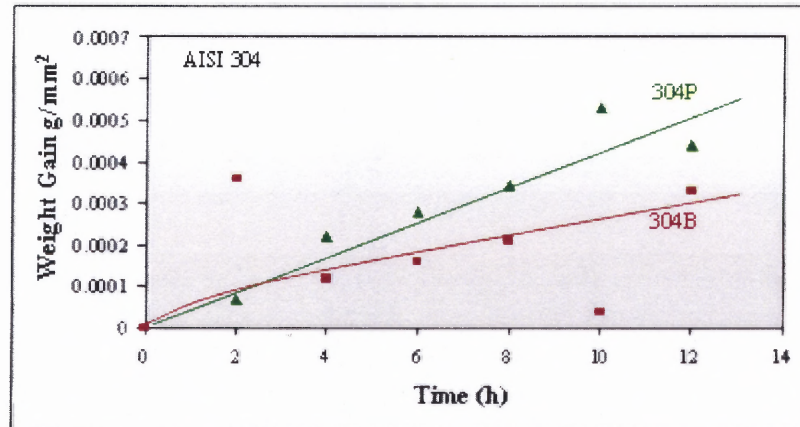


**Figure 6.18** The oxidation test of boronized and unboronized specimen (AISI 304) at 600 °C for 12 hours (B-boronized specimen, P-unboronized specimen).

## CHAPTER 7

### CONCLUSION

The boronized specimens of AISI 1018, AISI 4340, and AISI 304 were successfully prepared by the pack boronizing technique. The investigation of structure and properties of boride layer in ferrous alloys was concluded as followed:

1. AISI 1018, plain low carbon steel, showed the saw-tooth structure with the depth of about 75 – 76  $\mu\text{m}$ . The boride layer was consisted of an outer FeB phase layer and an inner Fe<sub>2</sub>B phase layer. The microhardness was obtained in the range of 1400-2200 HV.

2. Similar to AISI 1018, AISI 4340, high strength alloy steel, also demonstrated the saw-tooth structure with the depth of about 57 - 58  $\mu\text{m}$ . FeB and Fe<sub>2</sub>B phase were detected as a boride layer on the substrate. The microhardness was recorded in the range of 1800-2200 HV.

3. Unlike AISI 1018 and AISI 4340, the narrow and flatten boride layer (10 – 11  $\mu\text{m}$ ) was observed instead of the saw-tooth structure, as a result of alloying elements, particularly chromium and nickel in AISI 304. The microhardness of boride layer in AISI 304 was about 400-700 HV.

4. The new unique technique was used to evaluate the corrosion resistance and boronized sample steels showed the ability of the boronized coating to protect the substrate.

5. The boronized specimens also showed the improved of oxidation resistance at high temperature rather than the unboronized specimens.

## **CHAPTER 8**

### **FUTURE WORK**

Since the pack boronizing is the simplest boronizing technique to understand the basic principle required for advance research on developing boronized steel, other boronizing techniques are planned to study and yet realize the optimized properties.

1. The gas and plasma boronizing utilizes the gas medium, rather than the solid powder in the pack boronizing method, with appropriate and controllable procedures to produce the optimized properties.

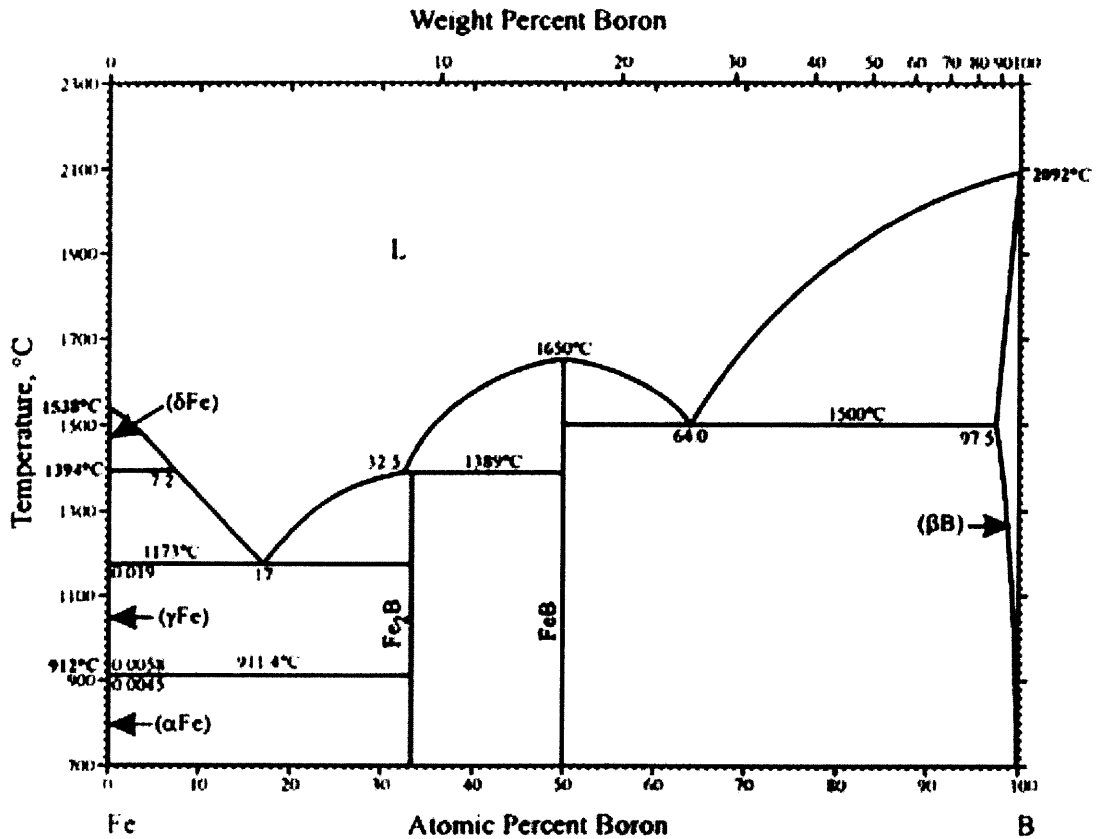
2. The multi-component boronizing is expected to construct the complex phase boride-layer that in general yields the desired properties.

3. The boronizing process for transition metals and their corresponding properties, which are deployed in extremely hard-surface applications, will be investigated.

## APPENDIX A

### B-Fe PHASE DIAGRAM

The binary diagram of Boron-Iron system is as followed:



P.K. Liao and K.E. Spear, *Phase Diagrams of Binary Iron Alloys*, H. Okamoto, ed., ASM International, Materials Park, OH, 41-47 (1993)

H. Okamoto, *J. Phase Equilibria*, 16(4), 364-365 (1995)

Figure A.1 B-Fe (Boron-Iron) phase diagram.

## APPENDIX B

### Fe<sub>2</sub>B XRD DATA

The crystallography data and XRD pattern of Fe<sub>2</sub>B are as followed:

#### Name and formula

Reference code:	00-003-1053
PDF index name:	Boron Iron
Empirical formula:	BFe <sub>2</sub>
Chemical formula:	Fe <sub>2</sub> B

#### Crystallographic parameters

Crystal system:	Tetragonal
Space group:	I4/mcm
Space group number:	140
a (Å):	5.0990
b (Å):	5.0990
c (Å):	4.2400
Alpha (°):	90.0000
Beta (°):	90.0000
Gamma (°):	90.0000
Volume of cell:	110.24
Z:	4.00
RIR:	-

#### Status, subfiles and quality

Status:	Marked as deleted by ICDD
Subfiles:	Inorganic Alloy, metal or intermetallic Common Phase
Quality:	Blank (B)

#### Comments

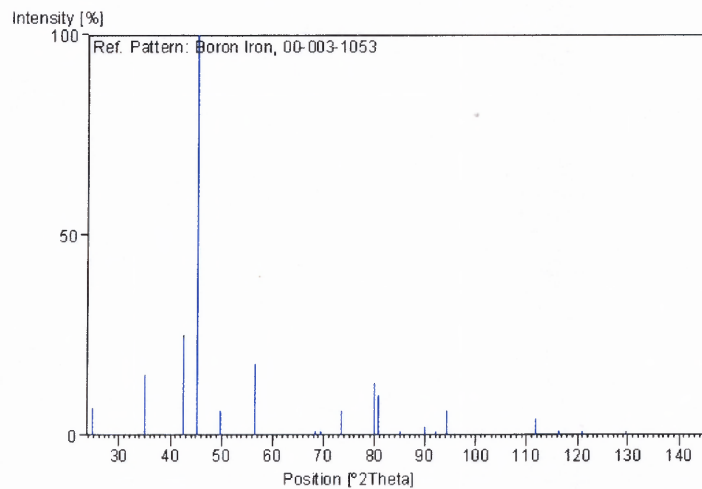
Deleted by: Deleted by 36-1332. Source of Unit Cell Data: powder diffraction.

#### References

Primary reference: The Dow Chemical Company., *Private Communication*

**Peak list**

No.	h	k	l	d [Å]	2Theta[deg]	I [%]
1	1	1	0	3.61000	24.641	7.0
2	2	0	0	2.56000	35.023	15.0
3	0	0	2	2.12000	42.612	25.0
4	2	1	1	2.01000	45.068	100.0
5	1	1	2	1.83000	49.787	6.0
6	2	0	2	1.63000	56.403	18.0
7	2	2	2	1.37000	68.425	1.0
8	3	2	1	1.35000	69.583	1.0
9	3	1	2	1.29000	73.330	6.0
10	2	1	3	1.20000	79.870	13.0
11	4	1	1	1.19000	80.678	10.0
12	4	2	0	1.14000	85.017	1.0
13	4	0	2	1.09000	89.934	2.0
14	0	0	4	1.07000	92.094	1.0
15	3	3	2	1.05000	94.381	6.0
16	4	1	3	0.93000	111.845	4.0
17	5	1	2	0.90700	116.268	1.0
18	3	1	4	0.88500	121.009	1.0
19	6	0	0	0.85100	129.692	1.0
20	5	3	2	0.80800	144.857	1.0

**Stick Pattern**



## APPENDIX C

### FeB XRD DATA

The crystallographic data and XRD pattern of FeB are as followed:

#### Name and formula

Reference code:	00-003-0957
PDF index name:	Boron Iron
Empirical formula:	BFe
Chemical formula:	FeB

#### Crystallographic parameters

Crystal system:	Orthorhombic
Space group:	Pbnm
Space group number:	62
a (Å):	4.0530
b (Å):	5.4950
c (Å):	2.9460
Alpha (°):	90.0000
Beta (°):	90.0000
Gamma (°):	90.0000
Measured density:	7.15
Volume of cell:	65.61
Z:	4.00
RIR:	-

#### Status, subfiles and quality

Status:	Marked as deleted by ICDD
Subfiles:	Inorganic Alloy, metal or intermetallic Common Phase
Quality:	Doubtful (O)

#### Comments

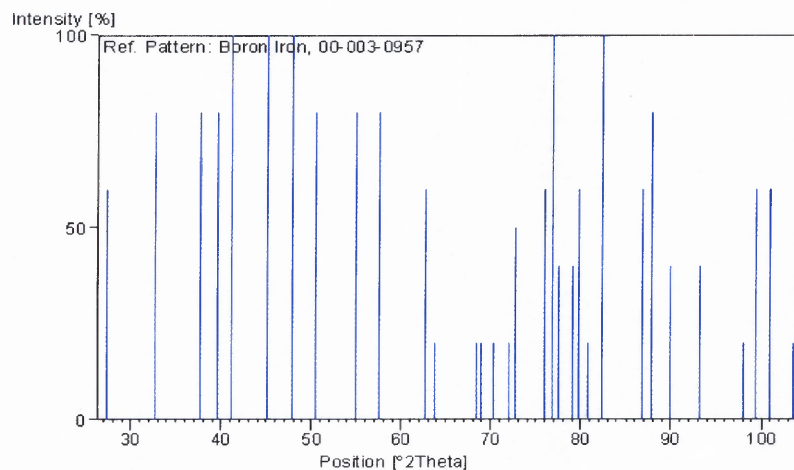
Deleted by:	Deleted by 32-463. Source of Unit Cell Data: powder diffraction.
Color:	Gray.

#### References

Primary reference:	Bjurstrom., <i>Ark. Kemi, Mineral. Geol.</i> , 11A
--------------------	--

**Peak list**

No.	h	k	l	d [Å]	2Theta[deg]	I [%]
1	1	1	0	3.26000	27.335	60.0
2	0	2	0	2.74000	32.655	80.0
3	1	0	1	2.38000	37.768	80.0
4	1	2	0	2.28000	39.492	80.0
5	1	1	1	2.19000	41.187	100.0
6	0	2	1	2.01000	45.068	100.0
7	2	1	0	1.90000	47.835	100.0
8	1	2	1	1.81000	50.375	80.0
9	1	3	0	1.67000	54.937	80.0
10	2	1	1	1.60000	57.559	80.0
11	0	0	2	1.48000	62.728	60.0
12				1.46000	63.687	20.0
13	0	4	0	1.37000	68.425	20.0
14	2	3	0	1.36000	68.999	20.0
15	1	1	2	1.34000	70.178	20.0
16	3	1	0	1.31000	72.033	20.0
17	1	4	0	1.30000	72.675	50.0
18				1.25000	76.084	60.0
19	1	2	2	1.24000	76.809	100.0
20	3	0	1	1.23000	77.549	40.0
21	3	2	0	1.21000	79.079	40.0
22	3	1	1	1.20000	79.870	60.0
23	1	4	1	1.19000	80.678	20.0
24				1.17000	82.352	100.0
25	3	2	1	1.12000	86.907	60.0
26				1.11000	87.889	80.0
27				1.09000	89.934	40.0
28	1	5	0	1.06000	93.221	40.0
29	3	3	1	1.02000	98.085	20.0
30				1.01000	99.401	60.0
31	2	3	2	0.99900	100.900	60.0
32				0.98100	103.482	20.0

**Stick Pattern**

## REFERENCES

1. Davis, J. R. (2002). Boriding. Surface Hardening of Steels - Understanding the Basics. Ohio:ASM International, 213-226.
2. Sinha, A. K. (1991). Boriding (Boronizing). Heat Treatment Vol.4, ASM Handbook. Ohio:ASM International, 437-447.
3. Stewart, K. (1997). Boronizing Protects Metals Against Wear. Adv. Mater. Process., 155(3), 23-25.
4. Kulka, M. & Pertek, A. (2003). Microstructure and properties of borided 41Cr4 steel after laser surface modification with re-melting. Appl. Surf. Sci., 214, 278-288.
5. Anthymidis, K.G., Stergioudis, E., & Tsipas, D.N. (2001). Boriding in a fluidized bed reactor. Mater. Lett., 51, 156-160.
6. Anthymidis, K.G., Zinoviadis, P., Roussos, D. & Tsipas, D.N. (2002). Boriding of nickel in a fluidized bed reactor. Mater. Res. Bull., 37, 515-522.
7. Anthymidis, K.G., Stergioudis, G., & Tsipas, D.N. (2002). Boride coatings on non-ferrous materials in a fluidized bed reactor and their properties. Sci. Technol. of Adv. Mater., 3, 303-311.
8. Bourithis, L., Papaefthymiou, S. & Papadimitriou, G.D. (2002). Plasma transferred arc boriding of a low carbon steel: microstructure and wear properties. Appl. Surf. Sci., 200, 203-218.
9. Bourithis, L. & Papadimitriou, G.D. (2003). Boriding a plain carbon steel with the plasma transferred arc process using boron and chromium diboride powders: microstructure and wear properties. Mater. Lett., 57, 1835-1839.
10. Yu, L.G., Khor, K.A. & Sundararajan, G. (2002). Boriding of mild steel using the spark plasma sintering (SPS) technique. Surf. Coat. Technol., 157, 226-230.
11. Cabeo, E.R., Laudien, G., Biemer, S., Rie, K. -T. & Hoppe, S. (1999). Plasma-assisted boriding of industrial components in a pulsed d.c. glow discharge. Surf. Coat. Technol. 116-119, 229-233.
12. Löbig, G. & Hunger, H. -J. (1997). Generation of boride layers on steel and nickel alloys by plasma activation of boron trifluoride. Thin Solid Films, 310, 244-250.

13. Bartsch, K. & Leonhardt, A. (1999). Formation of iron boride layers on steel by d.c.-plasma boriding and deposition processes. Surf. Coat. Technol., 116-119, 386-390.
14. Yoon, J. H., Jee, Y. K. & Lee, S.Y. (1999). Plasma paste boronizing treatment of the stainless steel AISI 304. Surf. Coat. Technol., 112, 71-75.
15. Davis, J.A., Wilbur, P.J., Williamson, D.L., Wei, R. & Vajo, J.J. (1998). Ion implantation boriding of iron and AISI M2 steel using a high-current density, low energy, broad-beam ion source. Surf. Coat. Technol., 103-104, 52-57.
16. Sen, U., Sen, S. & Yilmaz, F. (2004). Structural characterization of boride layer on boronized ductile irons. Surf. Coat. Technol., 176, 222-228.
17. Genel, K., Özbek, I., Kurt, A. & Bindal C. (2002). Boriding response of AISI W1 steel and use of artificial neural network for prediction of borided layer properties. Surf. Coat. Technol., 160, 38-43.
18. Özbek, I., Konduk, B.A., Bindal, C. & Ucisik A.H. (2002). Characterization of borided AISI 316L stainless steel implant. Vacuum, 65, 521-525.
19. Özbek, I. & Bindal, C. (2002). Mechanical properties of boronized AISI W4 steel. Surf. Coat. Technol., 154, 14-20.
20. Zakhariyev, Z., Marinov, M., Zlateva, R. & Khristov, KH. (1987). A new combination of coatings on carbide cutting tools. Surf. Coat. Technol., 31, 265-271.
21. Özbek, I., Akbulut, H., Zeytin, S., Bindal, C., & Ucisik, A.H. (2000). The characterization of borided 99.5% purity nickel. Surf. Coat. Technol., 126, 166-170.
22. Bindal, C. & Ucisik, A.H. (1999). Characterization of borides formed on impurity-controlled chromium-based low alloy steels. Surf. Coat. Technol., 122, 208-213.
23. Lee, S.Y., Kim, G.S. & Kim, B.-S. (2004). Mechanical properties of duplex layer formed on AISI 403 stainless steel by chromizing and boronizing treatment. Surf. Coat. Technol., 177-178, 178-184.
24. Maragoudakis, N.E., Stergioudis, G., Omar, H., Pavlidou, E. & Tspas, D.N. (2002). Boro-nitriding of steel US 37-1. Mater. Lett., 57, 949-952.
25. Gidikova, N. (1999). Vanadium boride coatings on steel. Mater. Sci. Eng. A, 278, 181-186.
26. Yan, P.X. & Su, Y.C. (1995). Metal surface modification by B-C-nitriding in a two-temperature-stage process. Mater. Chem. Phys., 39, 304-308.

27. Kulka M. & Pertek A. (2003). Characterization of complex (B + C + N) diffusion layers formed on chromium and nickel-based low-carbon steel. Appl. Surf. Sci., **218**, 114-123.
28. Pertek, A. & Kulka, M. (2003). Two-step treatment carburizing followed by boriding on medium-carbon steel. Surf. Coat Technol., **173**, 309-314.
29. Zakhariyev, Z. & Zlateva, R. (1993). Gas phase reactions during simultaneous boronizing and aluminizing of steels. J. Alloys Comp., **196**, 59-62.
30. Zlateva, R.S. & Zakhariyev, Z.T. (1993). Structure of boronizing layers on steels. Bulg. Chem. Comm., **26(1)**, 82-89.
31. Maragoudakis, N. E., Stergioudis, G., Omar, H., Paulidou, H. & Tsipas D.N. (2002). Boron–aluminide coatings applied by pack cementation method on low-alloy steels. Mater. Lett., **53**, 406-410.
32. Wierzchon, T., Bielinski, P. & Sikorski, K. (1995). Formation and properties of multicomponent and composite borided layers on steel. Surf. Coat. Technol., **73**, 121-124.
33. Dearnley, P. A. & Bell, T. (1985). Engineering the surface with boron based materials. Surface Engineering, **1(3)**, 203-217.
34. Chatterjee-Fischer, R. (1989). Boriding and Diffusion Metallizing. Surface Modification Technologies. New York:Marcel Dekker, Inc., 567-609.
35. Palombarini, G. and Carbucicchio, M. (1984). On the morphology of thermo-chemically produced Fe<sub>2</sub>B/Fe interfaces. J. Mater. Sci. Lett., **3**, 791-794.
36. Palombarini, G. and Carbucicchio, M. (1987). Growth of boride coatings on iron. J. Mater. Sci. Lett., **6**, 415-416.
37. Hunger, H. J. & Trute, G. (1994). Boronizing to Produce Wear-resistant Surface Layers. Heat Treatment of Metals, **2**, 31-39.
38. Budinski, K. (1988). Surface Engineering for Wear Resistance, Prentice-Hall, 303-345.
39. Skugorova, L. P., Shylkov, V.I. & Netschaev, A. I. (1972). Apparatus and technology of gas borating. Metalloved. Term. Obra. Met., **5**, 61-62.
40. Raveh A., Inspektor A., Carmi, U. & Avni R. (1983). Boronization of titanium and steels in a low pressure r.f. plasma. Thin Solid Film, **108**, 39-45.

41. Pasechnik, S.Y. *et al.* (1972). Protective Coatings on Metals, Vol.4. New York: Consultants Bureau, 37-40.
42. Kaidash, N.G. *et al.* (1972). Protective Coatings on Metals, Vol.4. New York: Consultants Bureau, 149-155.
43. Chatterjee-Fischer, R. (1981). Nitriding and nitrocarburizing Part V. Härt.-Tech. Mitt., 36 (5), 248-254.